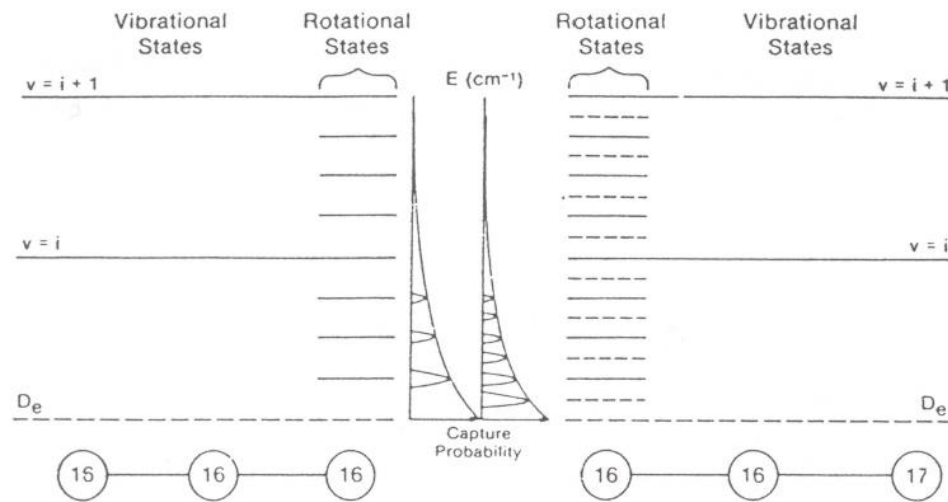


# Mass Independent Fractionation!

- Quantum mechanical ozone predissociation rotational state symmetry breaking:
  - Non-symmetric molecules have more rotational states



Schematic diagram of the process of inverse predissociation for  $O + O_2$  reaction. Note that the asymmetric isotopic species has double the number of rotational states and an increased probability of stabilization.

© source unknown. All rights reserved. This content is excluded from our Creative Commons license. For more information, see <http://ocw.mit.edu/fairuse>.

# Mass-Independent Fractionation

Mechanism: Available rotational states affect transition probability (Gao & Markus, 2002)

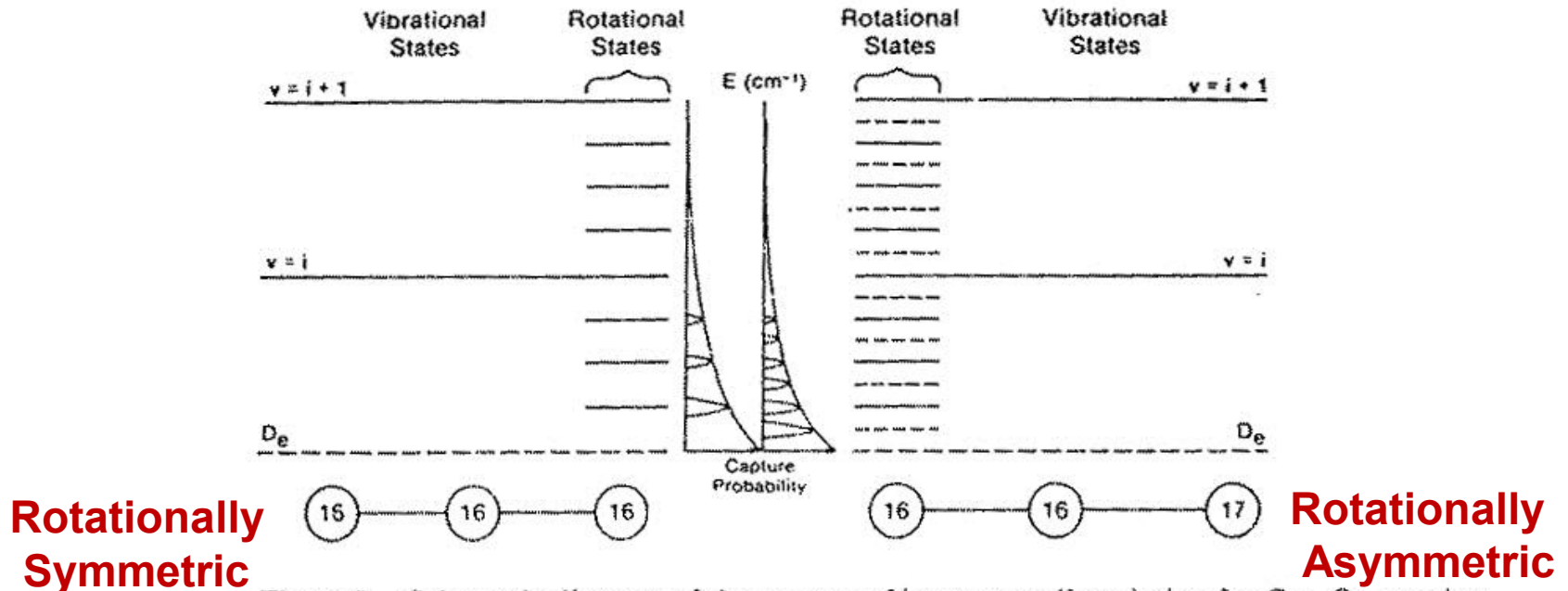


**Figure 8.** Schematic diagram of the process of inverse predissociation for  $O + O_2$  reaction. Note that the asymmetric isotopic species has double the number of rotational states and an increased probability of stabilization.

© source unknown. All rights reserved. This content is excluded from our Creative Commons license. For more information, see <http://ocw.mit.edu/fairuse>.

Molecular rotational symmetry is broken when  $^{18}O$  or  $^{17}O$  is substituted for  $^{16}O$  in  $O_2$  and  $O_3$  *doubling* the available quantum states available for transition.

# Babikov et al. (2003) cartoon summarizing their calculations

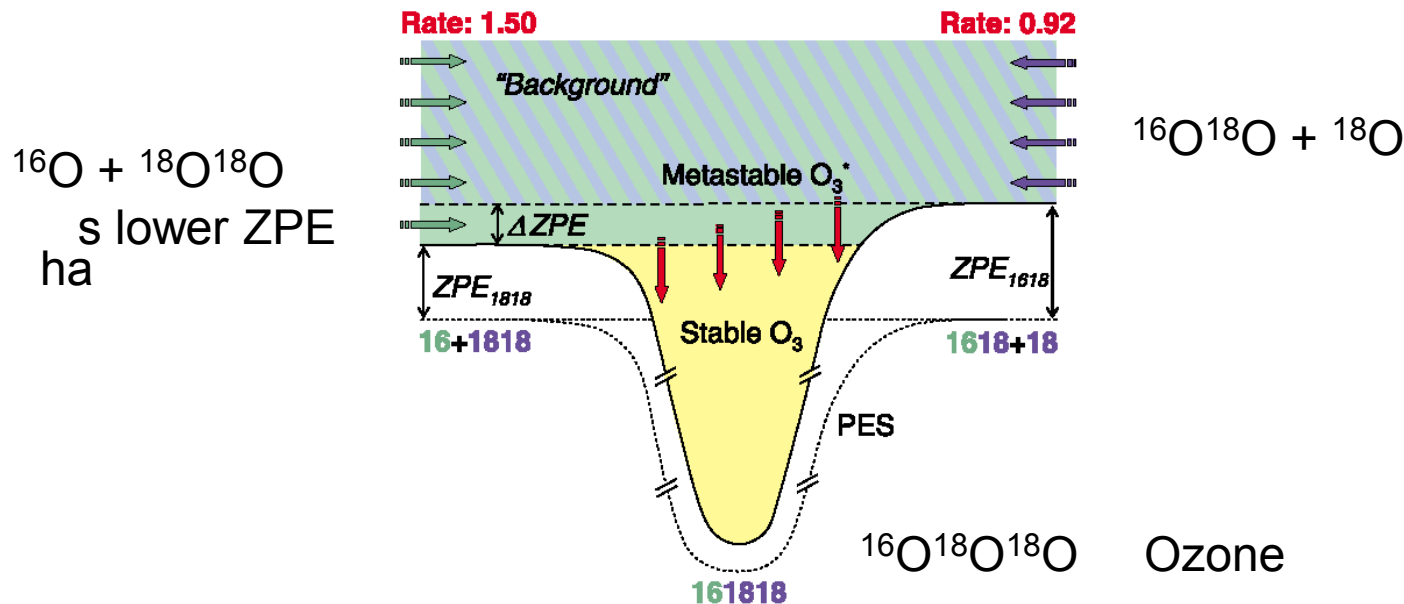


Fig. 2. Schematic for recombination processes forming ozone  $^{16}\text{O}^{18}\text{O}^{18}\text{O}$ . Stable ozone molecules are formed in the potential well (yellow part) as a result of collisional stabilization of metastable states formed above the well (in the green and striped blue/green part). The stabilization process is shown schematically as red descending arrows. Metastable states in the striped part of the spectrum can be formed from both entrance channels:  $^{16}\text{O} + ^{18}\text{O}^{18}\text{O}$  on the left (green arrows) and  $^{16}\text{O}^{18}\text{O} + ^{18}\text{O}$  on the right (blue arrows). Metastable states in the  $\Delta\text{ZPE}$  part of spectrum (green) are formed exclusively from the  $^{16}\text{O} + ^{18}\text{O}^{18}\text{O}$  entrance channel. The PES (dotted line) and the ZPE for both channels are shown (not to scale). Experimental relative rates of ozone formation for the two channels are given at the top.

© Elsevier. All rights reserved. This content is excluded from our Creative Commons license. For more information, see <http://ocw.mit.edu/fairuse>.

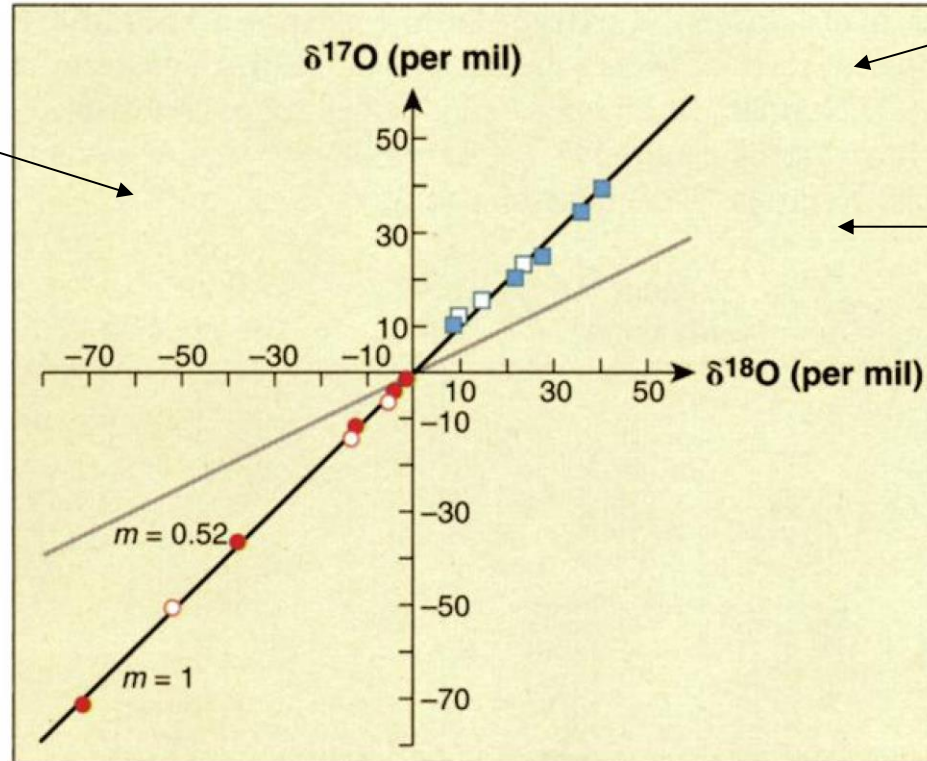
Source: Babikov, Dmitri, B. K. Kendrick, et al. "Quantum Origin of an Anomalous Isotope Effect in Ozone Formation." *Chemical Physics Letters* 372, no. 5 (2003): 686-91.

# Demonstration of “Mass-independent Fractionation” in the Laboratory

O<sub>3</sub> created in the lab from O<sub>2</sub>, via electric discharge (Thiemens & Heidenreich, 1983)

Later demonstrated in nature by high altitude

air samples (Thiemens et al., 1995)



m = 1.0

m ~ 0.52

Blue = O<sub>3</sub>  
Red = O<sub>2</sub>  
Two labs

**Plot of the first demonstration of a chemically produced mass independent isotope effect.** Square symbols, ozone samples; circles, molecular oxygen reservoirs;  $m = \delta^{17}\text{O}/\delta^{18}\text{O}$ . The report Gao and Marcus successfully explains these observations.

© AAAS. All rights reserved. This content is excluded from our Creative Commons license. For more information, see <http://ocw.mit.edu/fairuse>. Source: Thiemens, Mark H. "The Mass-Independent Ozone Isotope Effect." *Science* 293, no. 5528 (2001): 226.

# Mass-independent Fractionation of Oxygen in the Stratosphere

Can define anomalous  $^{17}\text{O}$  signal as:

$$\Delta^{17}\text{O} = \delta^{17}\text{O} - 0.52\delta^{18}\text{O}$$

average air used as standard, reported as parts per meg (1 in  $10^6$ )

empirically determined

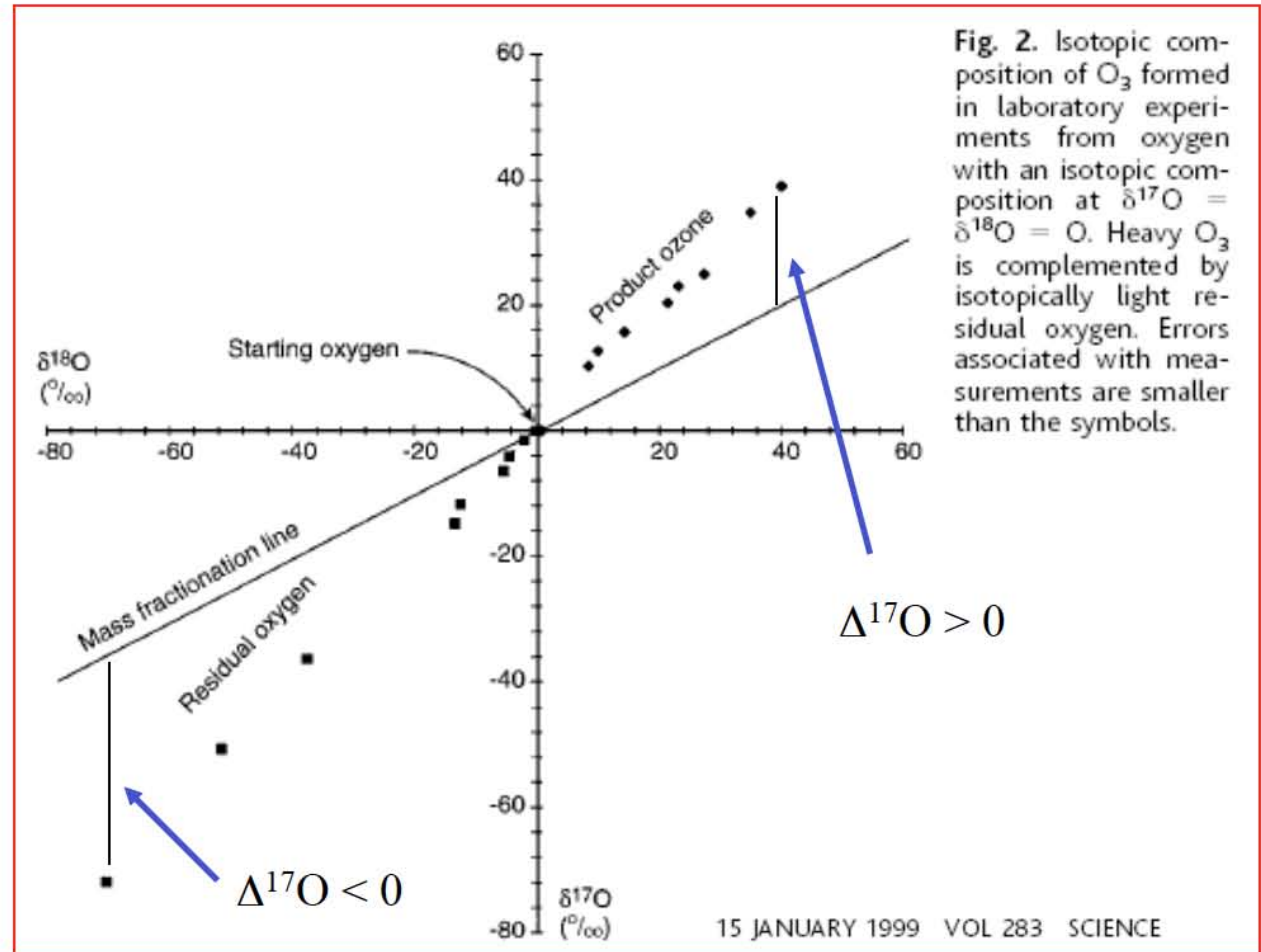


Fig. 2. Isotopic composition of  $\text{O}_3$  formed in laboratory experiments from oxygen with an isotopic composition at  $\delta^{17}\text{O} = \delta^{18}\text{O} = 0$ . Heavy  $\text{O}_3$  is complemented by isotopically light residual oxygen. Errors associated with measurements are smaller than the symbols.

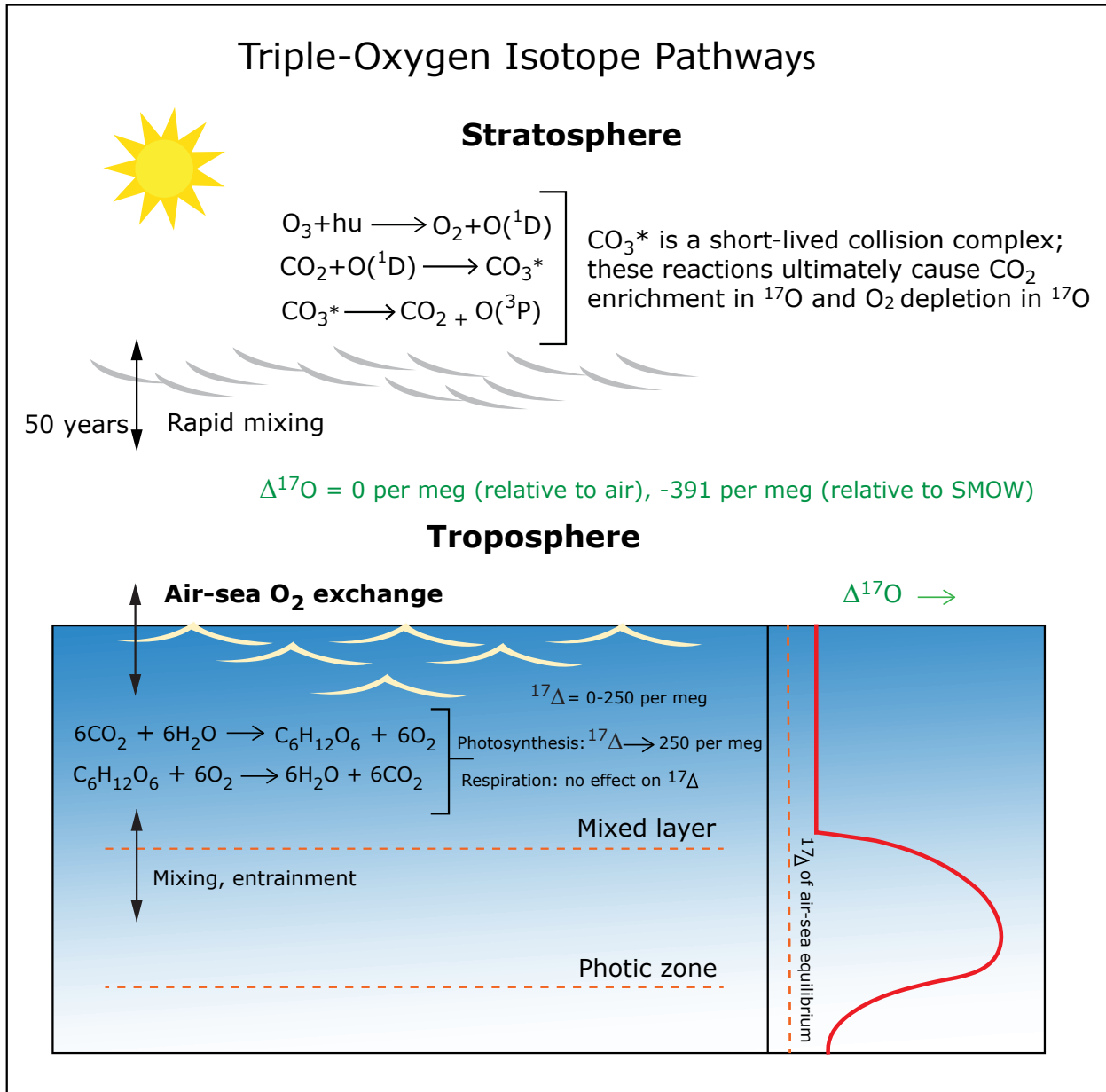
Thiemens and Heidenreich, 1983; Thiemens, 1999 (review)

© AAAS. All rights reserved. This content is excluded from our Creative Commons license. For more information, see <http://ocw.mit.edu/fairuse>. Source: Thiemens, Mark H. "Mass-Independent Isotope Effects in Planetary Atmospheres and the Early Solar System." *Science* 283, no. 5400 (1999): 341-5.

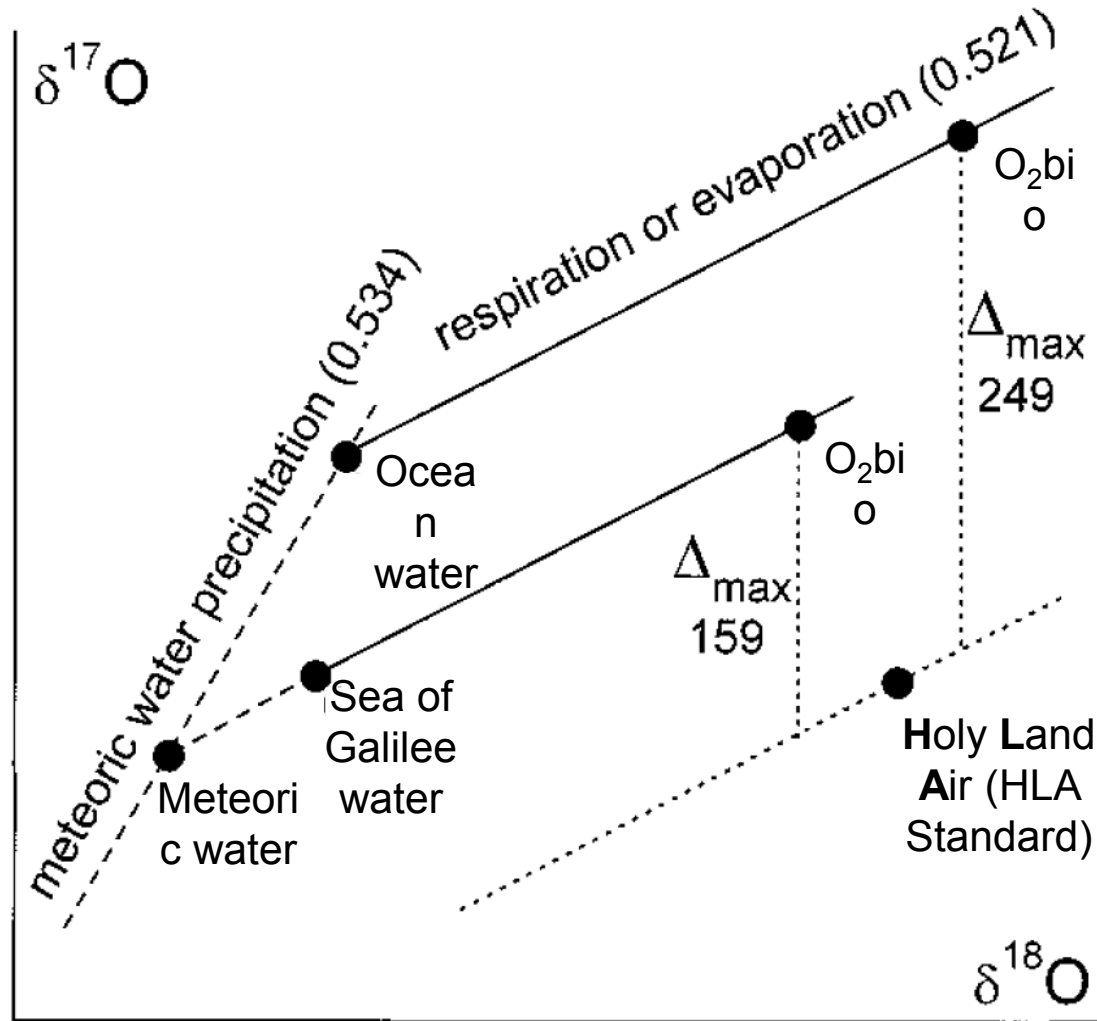
# Primary Production

- Gross primary production
  - Total amount of carbon fixed per unit time
- Net primary production
  - Net carbon fixed (gross minus respiration/dark)
- Net community production
  - That net biomass production
- New production
  - Production arising from influx of new nitrate
    - Dugdale & Goering (1967) L&O v12 p196
    - f-ratio = New/Net
      - Varies from 0.05 to 0.5 (oligotrophic → eutrophic)
  - Eppley & Peterson (1979) Nature v282 p677
- Export production
  - Flux of carbon leaving euphotic zone
    - e-ratio = Export/Net ~ f-ratio

# Triple-Oxygen Isotope Pathways



# Schematic Oxygen Isotope Relationships



© AAAS. All rights reserved. This content is excluded from our Creative Commons license. For more information, see <http://ocw.mit.edu/fairuse>.

Source: Luz, Boaz, and Eugeni Barkan. "Assessment of Oceanic Productivity with the Triple-Isotope Composition of Dissolved Oxygen." *Science* 288, no. 5473 (2000): 2028-31.

# Remember – Mass-Dependent Fractionation:

## Equilibrium Fractionation:

$$\alpha_{2/1} = (\alpha_{3/1})^\beta \quad \text{with} \quad \beta = (1/m_1 - 1/m_2) / (1/m_1 - 1/m_3)$$

with  $m_1 = {}^{32}\text{S}$  (31.97207070),  $m_2 = {}^{33}\text{S}$  (32.97145854),  $m_3 = {}^{34}\text{S}$  (33.9678665),  $m_4 = {}^{36}\text{S}$  (35.96708062)

$$\beta = 0.5158_8$$

## Kinetic Fractionation:

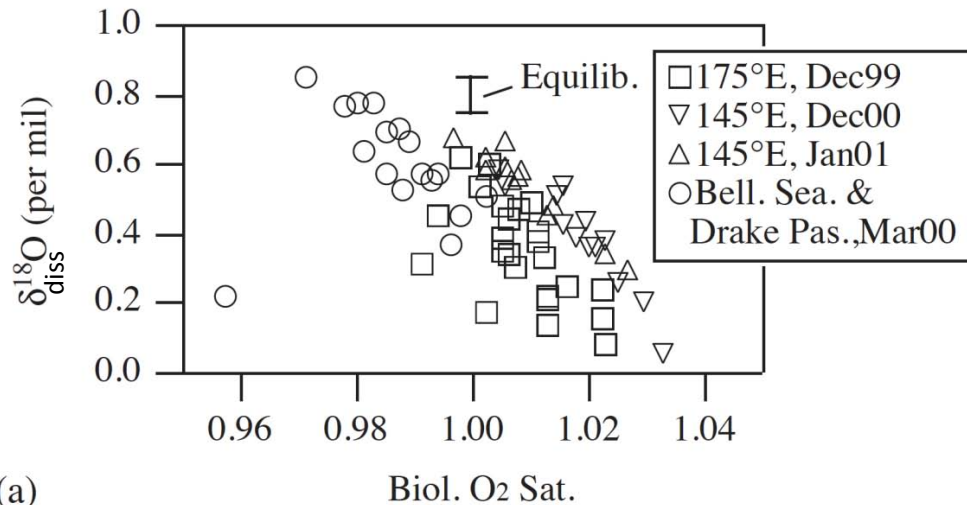
$$\alpha_{2/1} = (\alpha_{3/1})^\beta \quad \text{with} \quad \beta = [\ln (m_1/m_2)] / [\ln (m_1/m_3)]$$

with  $m_1 = {}^{32}\text{S}$  (31.97207070),  $m_2 = {}^{33}\text{S}$  (32.97145854),  $m_3 = {}^{34}\text{S}$  (33.9678665),  $m_4 = {}^{36}\text{S}$  (35.96708062)

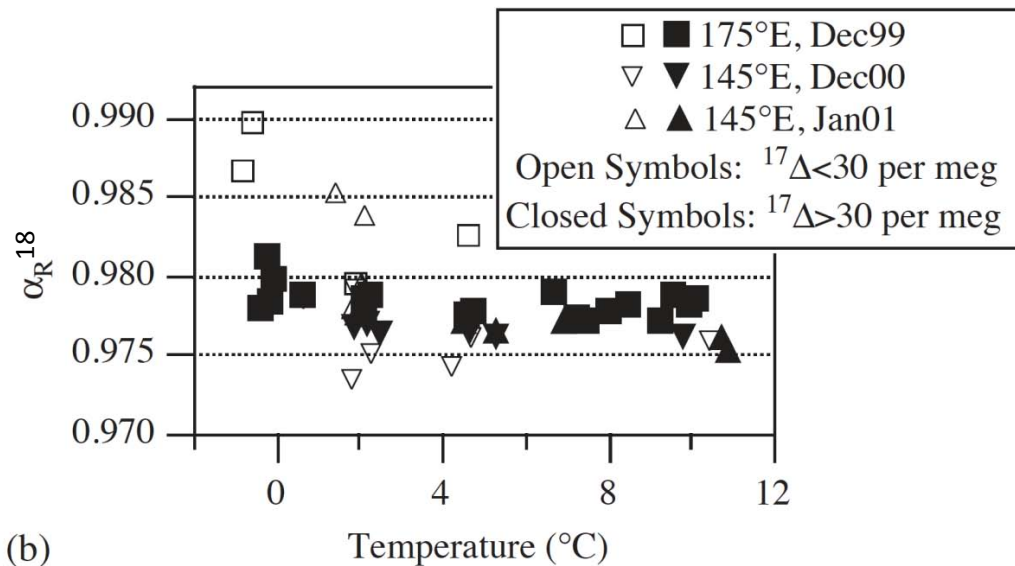
$$\beta = 0.5083_1$$

*Ref.: Young ED, A Galy, H Nagahara, 2002, Kinetic and equilibrium mass-dependent isotope fractionation laws in nature and their geochemical and cosmochemical significance, GCA 66 (6), 1095-1104.*

# Isotope Fractionation during Respiration

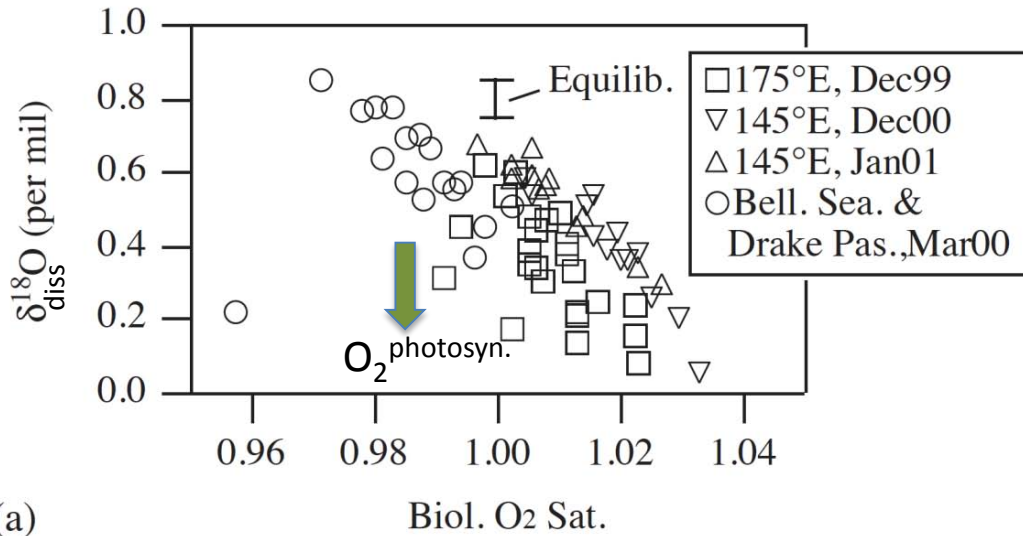


Equilibrium refers to  $\delta_{\text{sat}}^{18}\text{O}$  at surface temperatures of the study region (Southern Ocean) = + 0.8 per mil

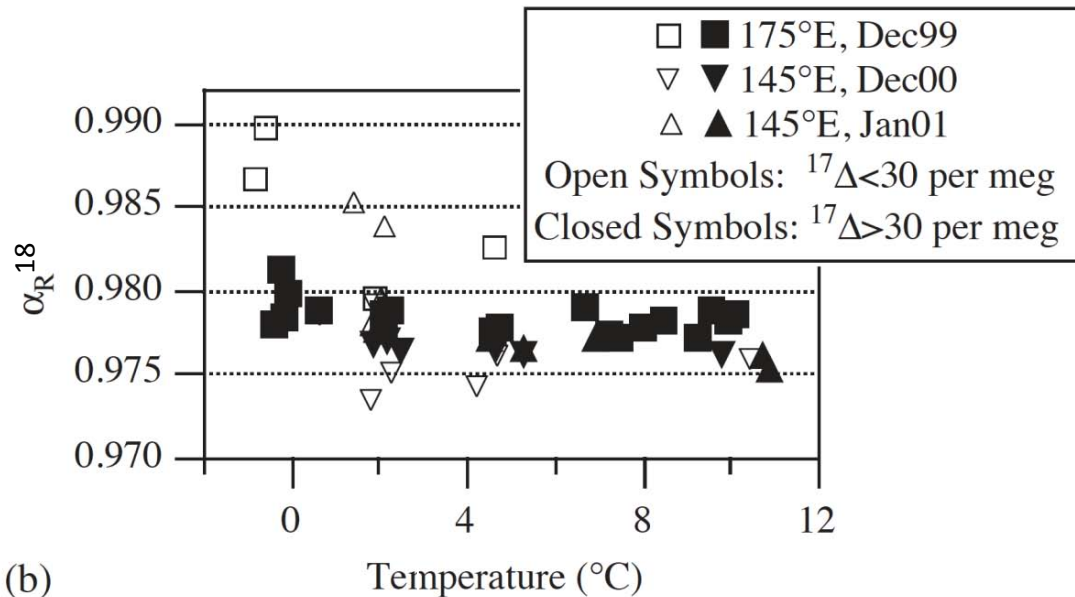


© Elsevier. All rights reserved. This content is excluded from our Creative Commons license. For more information, see <http://ocw.mit.edu/fairuse>. Source: Hendricks, Melissa B., Michael L. Bender, et al. "Net and Gross O<sub>2</sub> Production in the Southern Ocean from Measurements of Biological O<sub>2</sub> Saturation and its Triple Isotope Composition." *Deep Sea Research Part I: Oceanographic Research Papers* 51, no. 11 (2004): 1541-61.

# Isotope Fractionation during Respiration



(a)



(b)

## Photosynthetic O<sub>2</sub>:

$\delta^{18}\text{O}$  of atmospheric O<sub>2</sub> w.r.t SMOW is +23.5 per mil (Kroopnick & Graig, 1972) – i.e. *Dole Effect*.

--Then – relative to air:

$$\delta^{18}\text{O}_{\text{SMOW}} = (X^{18}_{\text{SMOW}}/X^{18}_{\text{atm}} - 1) 10^3 = -22.96$$

--Note that for small  $^{17}\Delta$  values, N/G, and thus  $\alpha^{18}_{\text{R}}$  is not well constrained.

## Definitions:

$$\Delta^{17}\text{O} = \ln(X^{17}/X^{17}_{\text{std}}) - 0.516 (X^{18}/X^{18}_{\text{std}}) 10^6$$

or

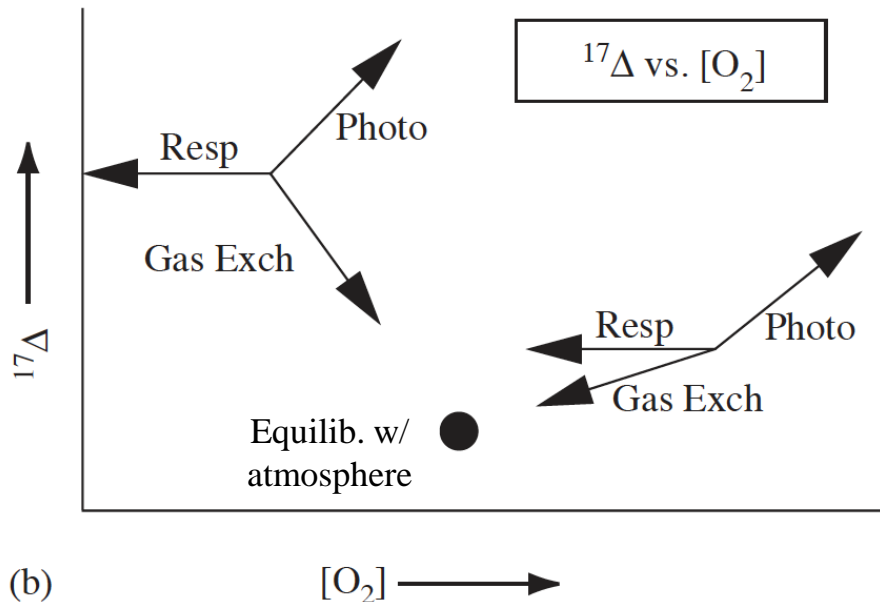
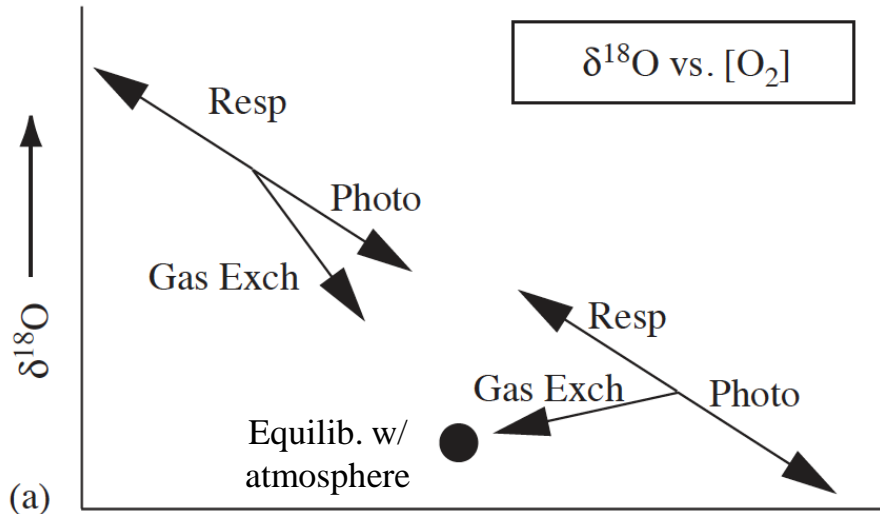
$$\Delta^{17}\text{O} = \ln(\delta^{17}\text{O}/10^3 + 1) - 0.516 \ln(\delta^{18}\text{O}/10^3 + 1) 10^6$$

or

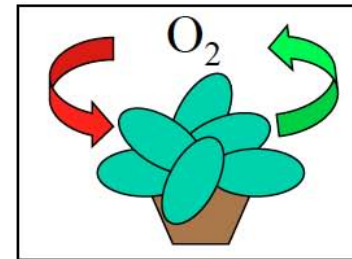
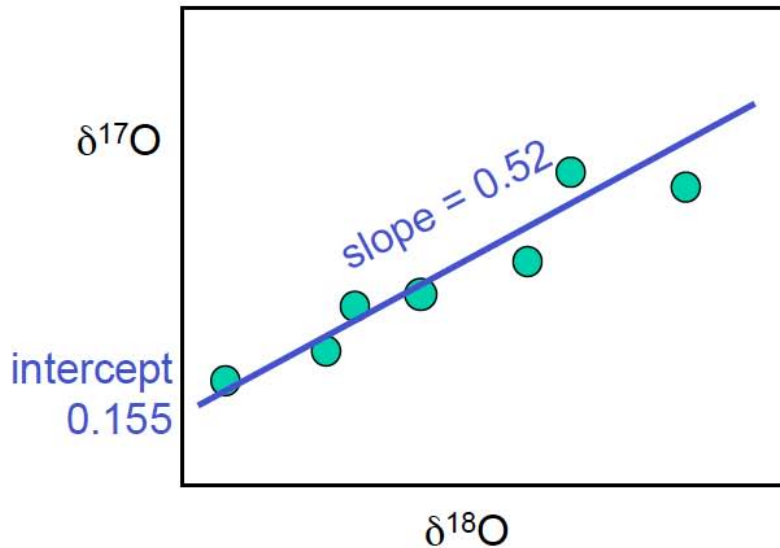
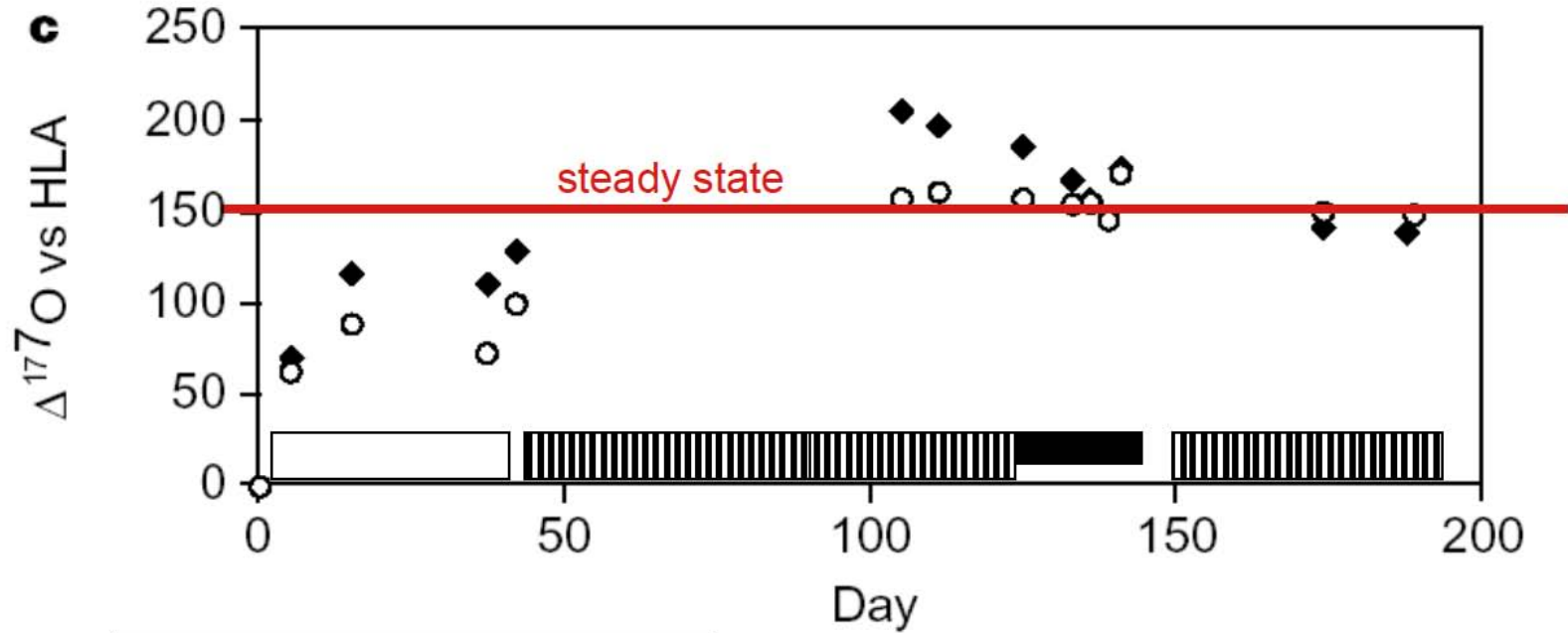
$$\Delta^{17}\text{O} = (\delta^{17}\text{O} - 0.516 \delta^{18}\text{O}) 10^3$$

Note: the slope in  $\delta^{17}\text{O}$  vs.  $\delta^{18}\text{O}$  space varies between studies from 0.516 to 0.521. It is chosen so that  $\Delta^{17}\text{O}$  is insensitive to respiration.

Because variations are so small, differences are expressed as parts per million (per meg).



# Closed biological system – steady state $\Delta^{17}\text{O}$ (wrt air)



**Luz and Barkan, 2000**

# Schematic Oxygen Isotope Relationships in the Mixed Layer

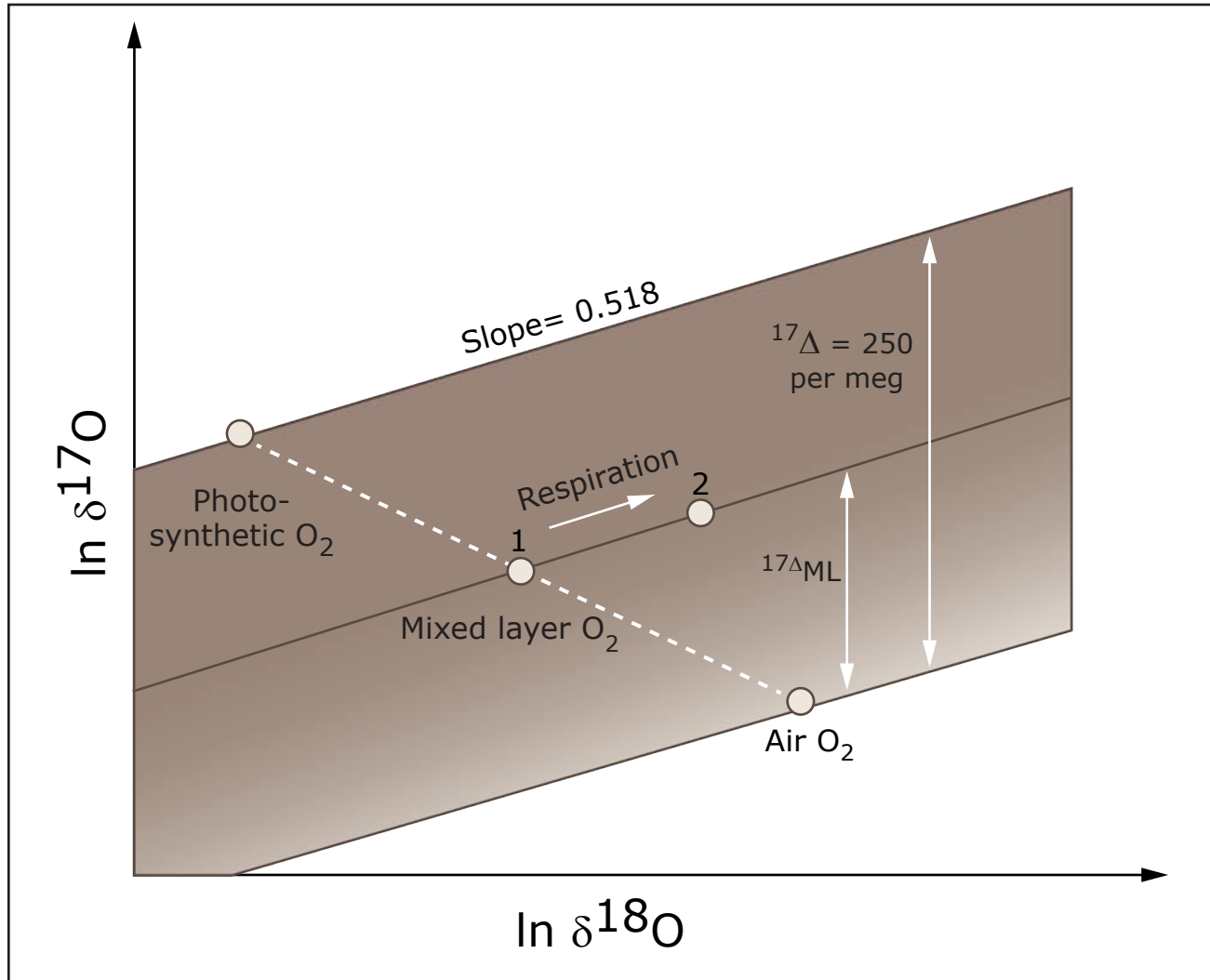


Image by MIT OpenCourseWare.

# Oxygen Concentration in the Mixed Layer

$O_2$  concentration = Gross  $O_2$  production – Respiration + Gas exchange

$$h \, dC/dt = G - R + k (C_{\text{sat}} - C)$$

$G$  = Gross  $O_2$  production by photosynthesis (e.g. in  $\text{mmol } O_2 \text{ m}^{-2} \text{ d}^{-1}$ )

$R$  =  $O_2$  consumption by respiration

$h$  = Average height of mixed layer

$C$  = Concentration;  $_{\text{sat}}$  = at saturation (e.g. in  $\text{mmol } O_2 \text{ m}^{-3}$ )

$k$  = Gas exchange coefficient for  $O_2$  ( $\text{m d}^{-1}$ ), proxy: Ar

For the isotopomers  $^{17}O^{16}O$  and  $^{18}O^{16}O$  dissolved in the mixed layer, we introduce the isotope ratio  $X_{\text{diss}}$  and the fractionation factors for photosynthesis  $\alpha_P$  and respiration  $\alpha_R$ . Subscripts  $_w$  and  $_{\text{sat}}$  denote isotope ratios of oxygen in seawater ( $H_2O$ ) and dissolved  $O_2$  in equilibrium with the atmosphere, respectively. Then:

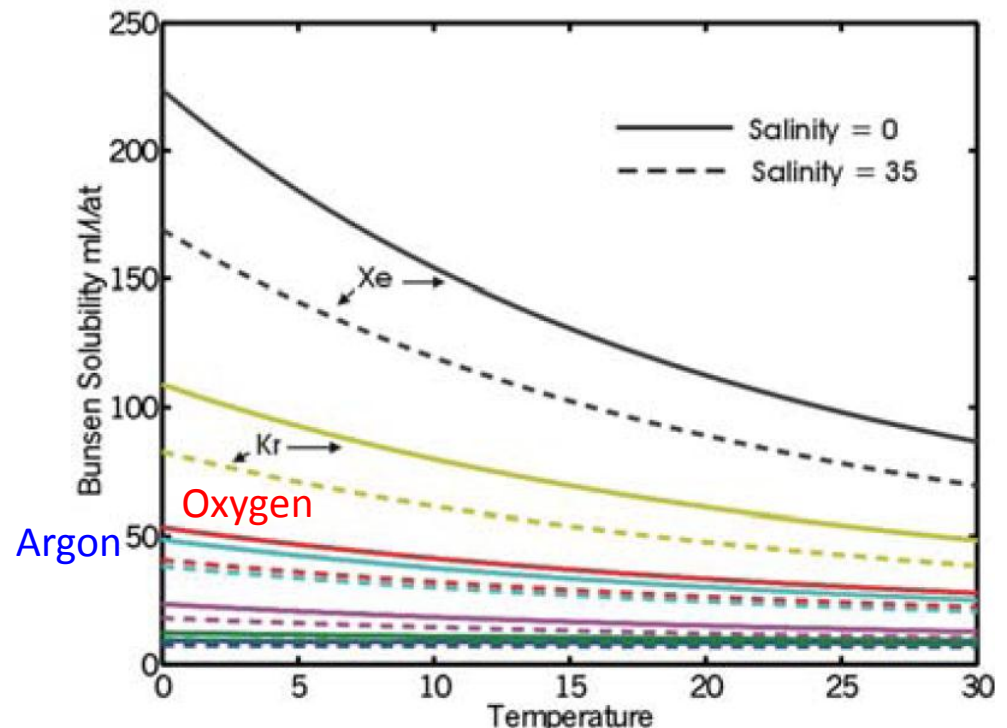
$$h \, d(CX_{\text{diss}})/dt = GX_w \alpha_P - RX_{\text{diss}} \alpha_R + k (C_{\text{sat}} X_{\text{sat}} - CX_{\text{diss}})$$

$= 1$

# Gas Solubility

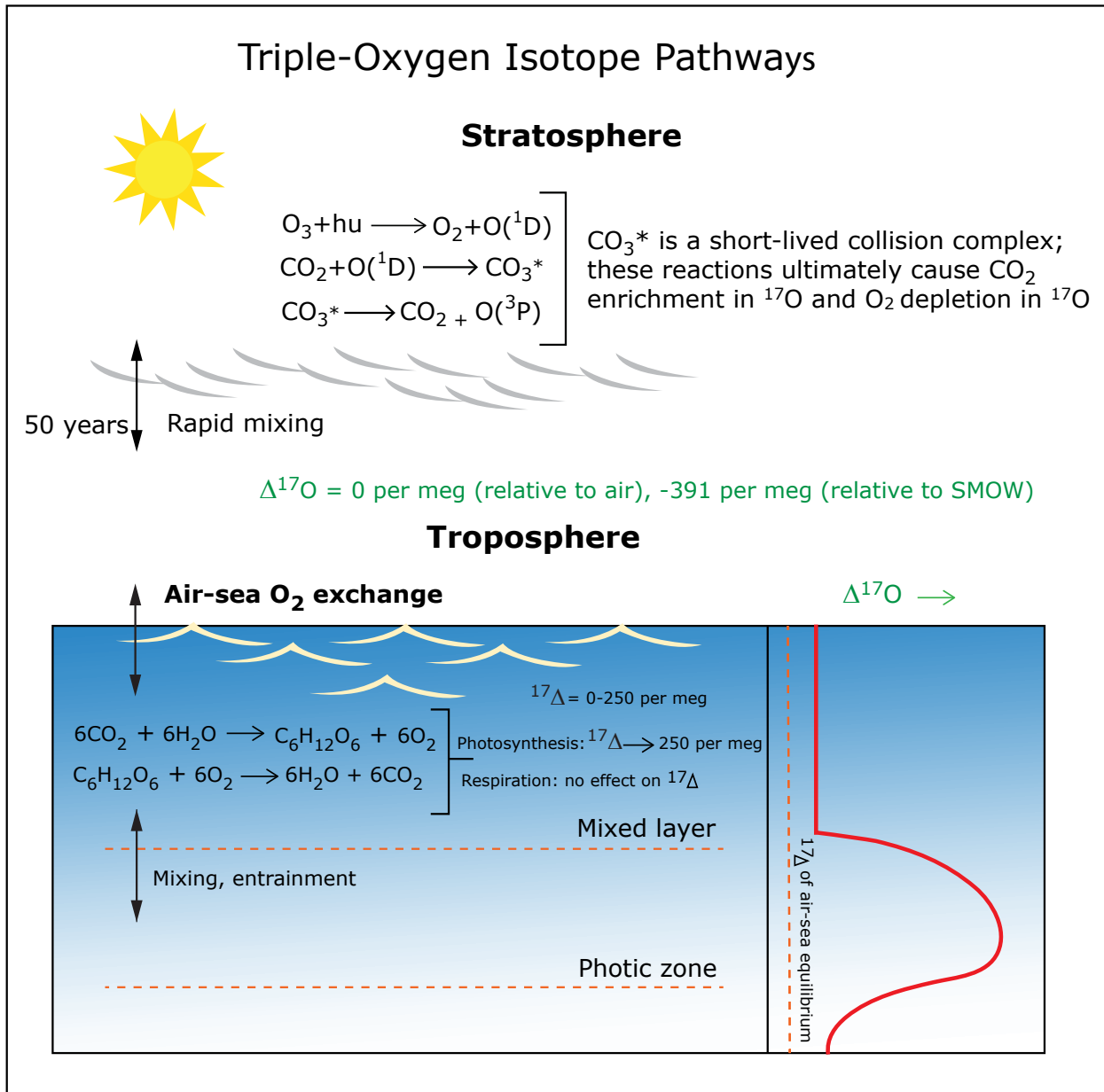
- Gas solubility generalities:
  - heavier, more polar gases are more soluble
  - all gases are more soluble at **lower** temperatures\*
    - more soluble gases have greater temperature dependence
  - salinity depresses solubility

Note the similarity in solubility between oxygen and argon



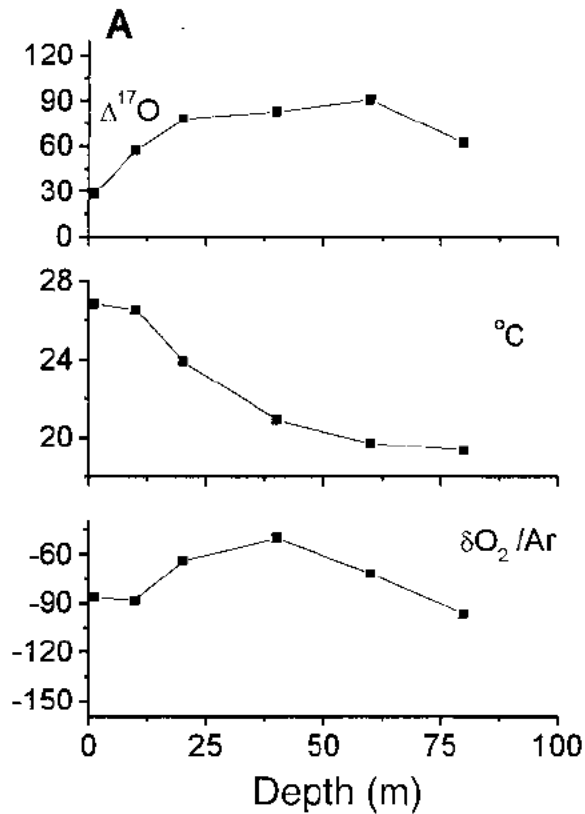
© source unknown. All rights reserved. This content is excluded from our Creative Commons license. For more information, see <http://ocw.mit.edu/fairuse>.

# Triple-Oxygen Isotope Pathways

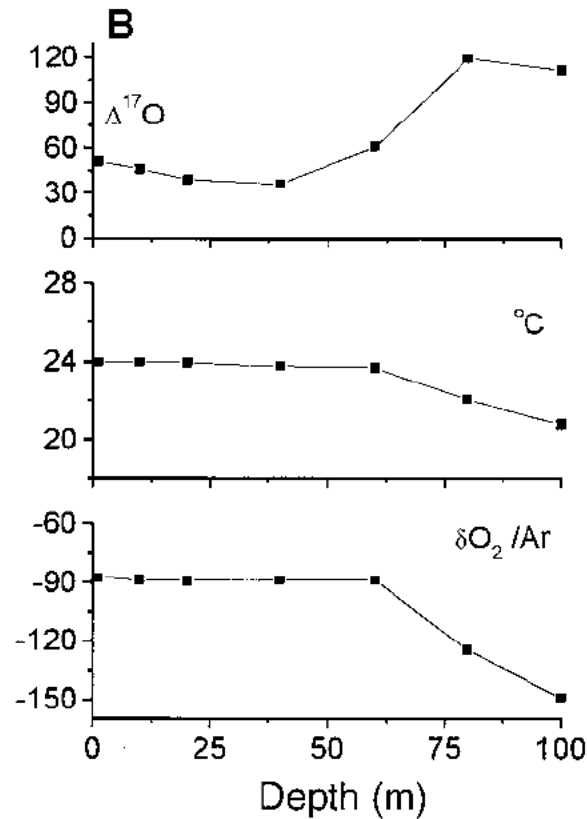


# Triple-Oxygen, Temperature and $O_2/Ar$ at Bermuda (BATS)

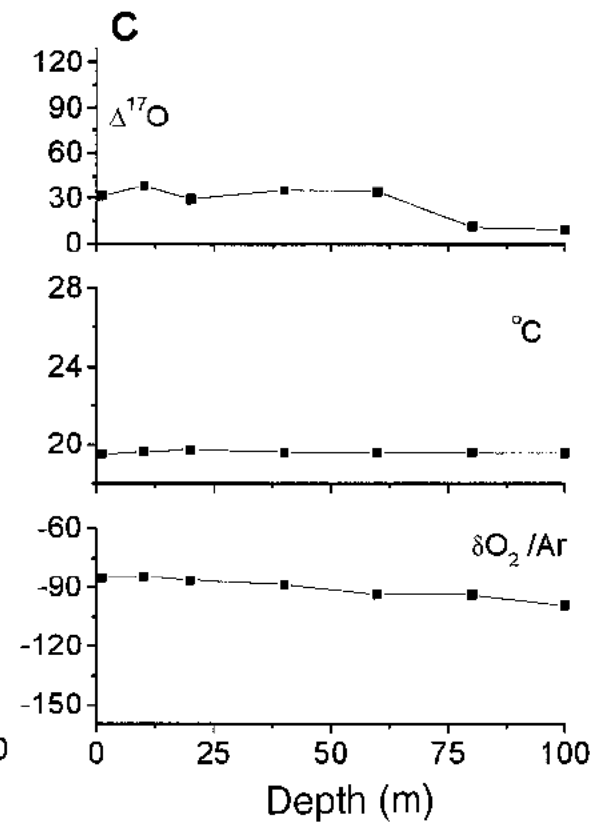
7 July 1998



7 November 1998



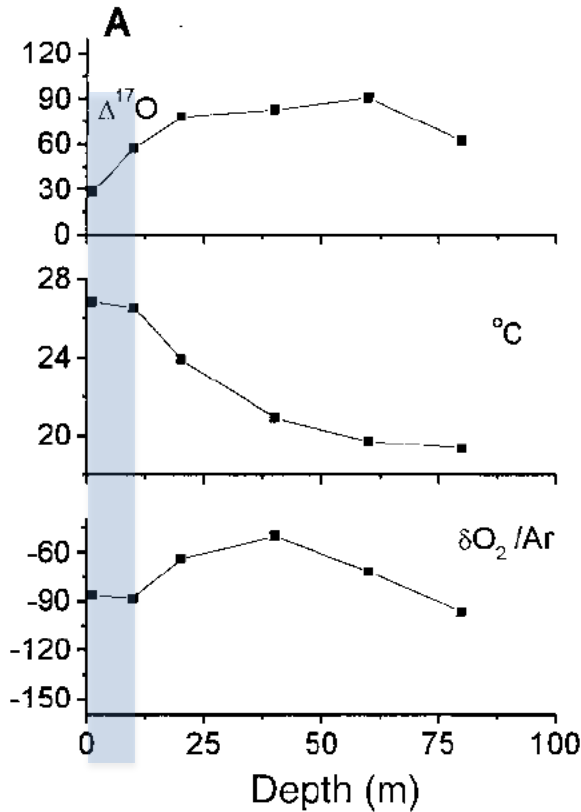
23 March 1999



© AAAS. All rights reserved. This content is excluded from our Creative Commons license. For more information, see <http://ocw.mit.edu/fairuse>. Source: Luz, Boaz, and Eugeni Barkan. "Assessment of Oceanic Productivity with the Triple-Isotope Composition of Dissolved Oxygen." *Science* 288, no. 5473 (2000): 2028-31.

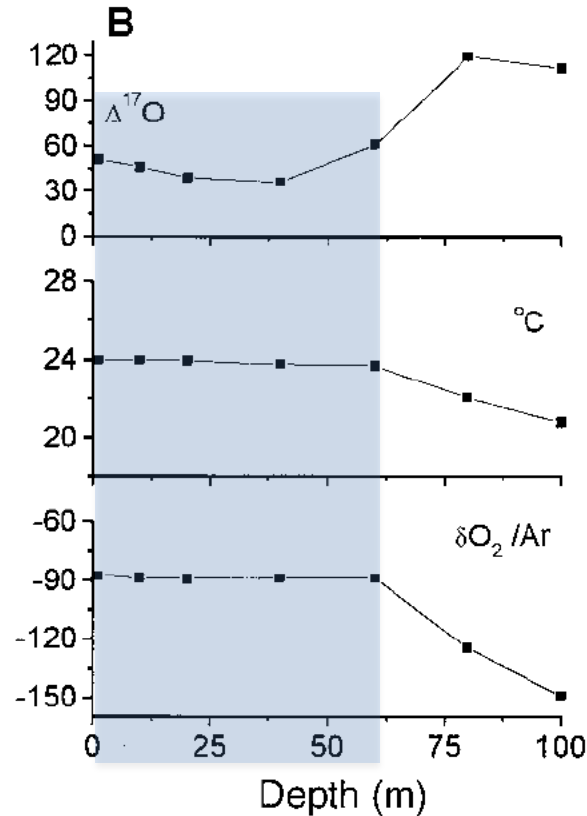
# Triple-Oxygen, Temperature and $O_2/Ar$ at Bermuda (BATS)

7 July 1998



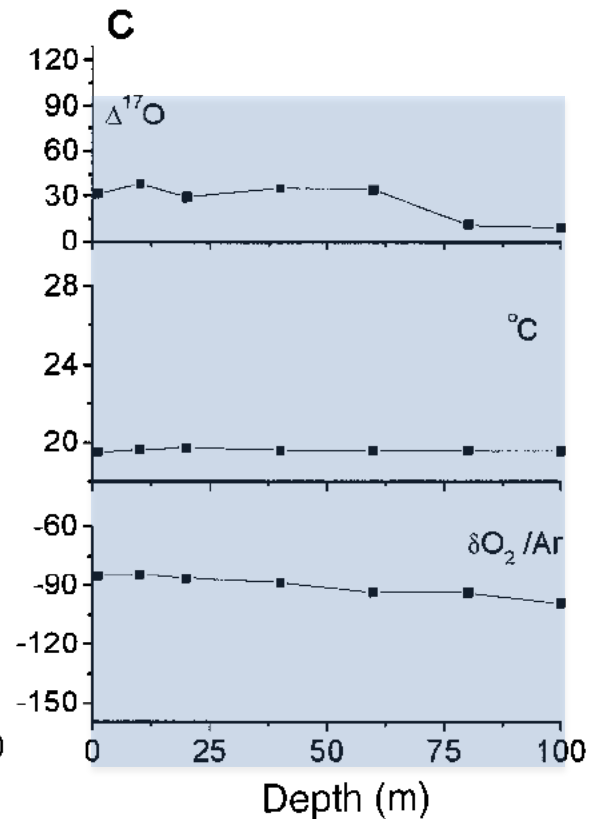
Thermocline  $O_2$  max due to net accumulation of  $O_2^{photosyn}$

7 November 1998



In situ  $O_2$  production, but uptake > production

23 March 1999



Mixed layer > photic zone  
No photosyn. in thermocline

$$h d(CX_{diss})/dt = GX_w \alpha_P - RX_{diss} \alpha_R + k (C_{sat} X_{sat} - CX_{diss})$$

=1

By replacing  $R$  with  $G + k (C_{sat} \dots C)$  and dividing each side by  $X_{std}$ , the isotope ratio of the standard (atmospheric  $O_2$ ), we can express  $\delta_{diss}O$  as a function of  $G/kC$ ,  $C/C_{sat}$  and  $\alpha_R$  according to:

$$\delta_{dis}O / 10^3 = \frac{\{(G/kC_{sat}) (\delta_w O/10^3 + 1) + (\delta_{sat} O/10^3 + 1)\}}{\{(G/kC_{sat}) + 1 - [(G/kC_{sat}) + 1 - (C/C_{sat})] (1 - \alpha_R)\}} - 1$$

This equation can also be expressed in terms of the ratio of net  $O_2$  production ( $N$ ) to gross  $O_2$  production ( $G$ ),  $C/C_{sat}$  and  $\alpha_R$ :

$$\delta_{dis}O / 10^3 = \frac{\{(C/C_{sat} - 1) (\delta_w O/10^3 + 1) + (N/G) (\delta_{sat} O/10^3 + 1)\}}{\{(C/C_{sat}) - 1 + (N/G) - [1 - (N/G)] [(C/C_{sat}) - 1] (1 - \alpha_R)\}} - 1$$

Melissa Hendricks and colleagues (*Deep-Sea Res. 1*, 51, 1541-1561, 2004) derive equivalent equations for expressions of  $\Delta^{17}O_{dis}$  in the appendix of their paper, e.g.

$$N/G = (C/C_{sat} - 1) (\Delta^{17}O_{diss} - \Delta^{17}O_w) / (\Delta^{17}O_{sat} - \Delta^{17}O_{dis})$$

# Triple-Isotope Measurements of Dissolved Oxygen Since 2000

World map with locations where the triple isotopic composition of dissolved oxygen has been used to assess marine productivity has been removed due to copyright restrictions.

See figure 1 in Juranek, L. W., and P. D. Quay. ["Using Triple Isotopes of Dissolved Oxygen to Evaluate Global Marine Productivity."](#) *Annual Review of Marine Science* 5 (2013): 503-524.

Table with summary of previously published comparisons of various quantities has been removed due to copyright restrictions.

See table 1 in Juranek, L. W., and P. D. Quay. ["Using Triple Isotopes of Dissolved Oxygen to Evaluate Global Marine Productivity."](#) *Annual Review of Marine Science* 5 (2013): 503-24.

# Comparison of Primary Production and Gross Oxygen Production Methods

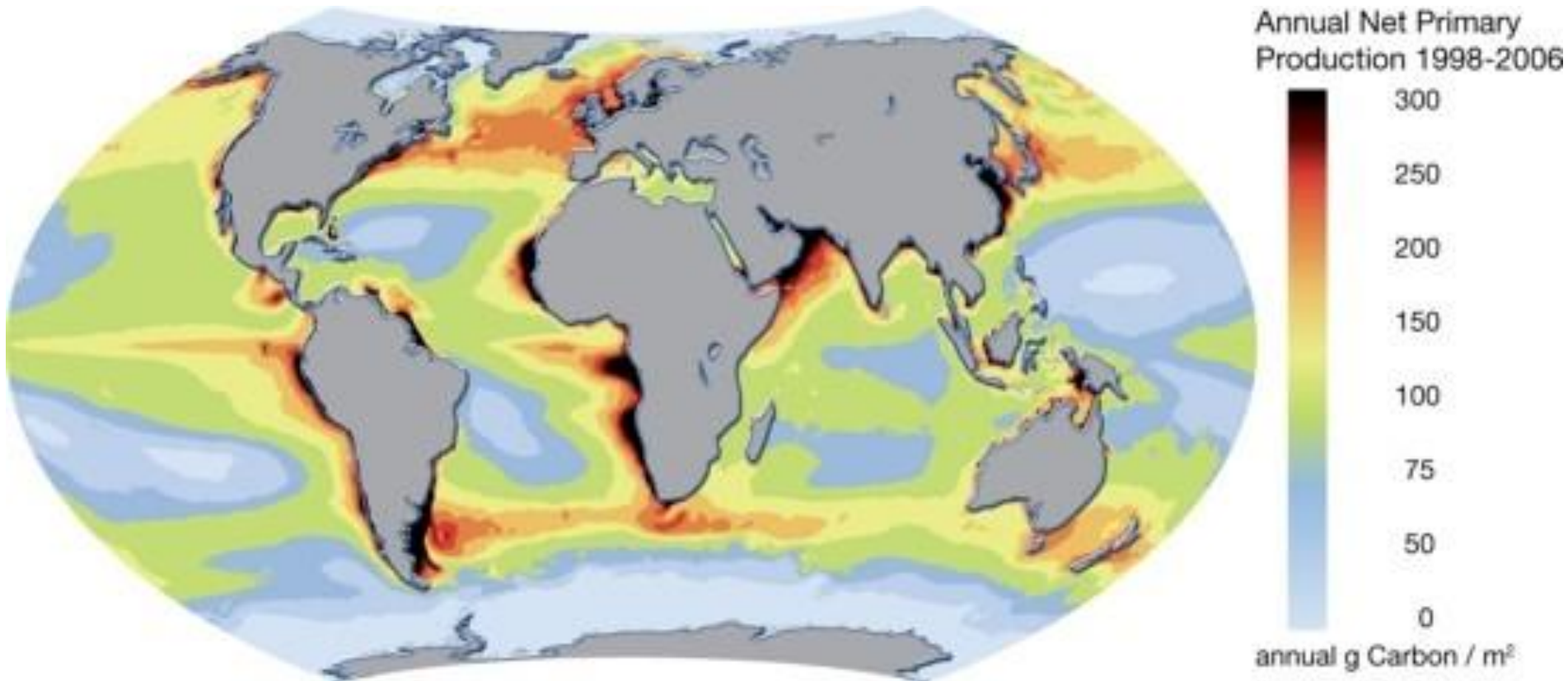
Table with summary of previously published comparisons of various quantities has been removed due to copyright restrictions.

See table 1 in Juranek, L. W., and P. D. Quay. "[Using Triple Isotopes of Dissolved Oxygen to Evaluate Global Marine Productivity.](#)" *Annual Review of Marine Science* 5 (2013): 503-24.

# Satellite-based Primary Production Estimates

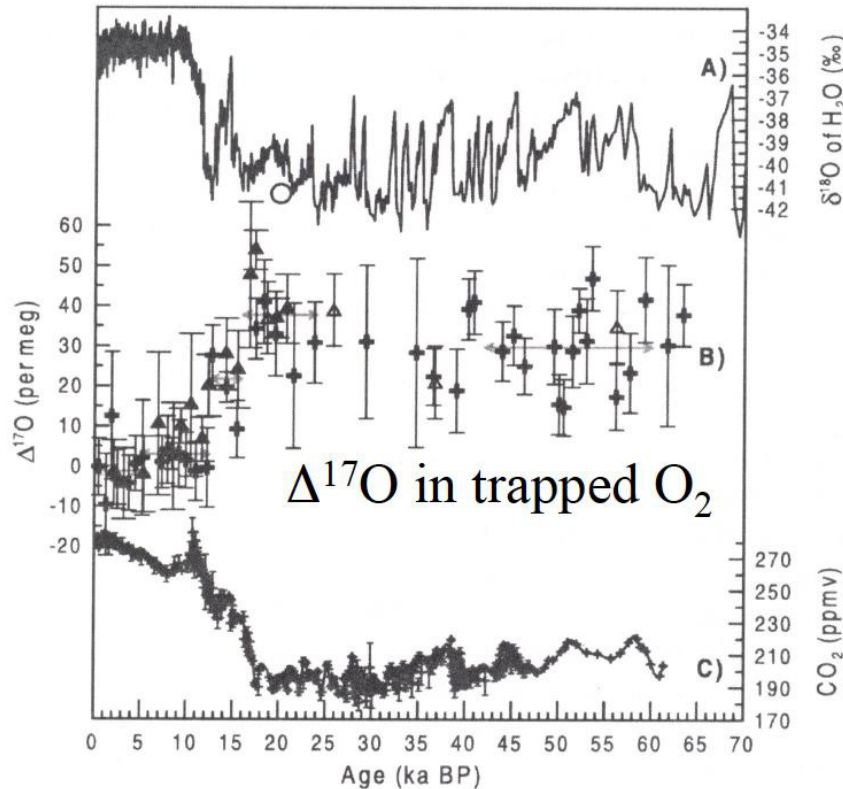
VGPM = Vertically Generalized Productivity Model (Behrenfeld & Falkowski, 1997)

CbPM = C-based Productivity Model (Behrenfeld et al., 1995, Westberry et al., 2008)



Courtesy of [Hugo Ahlenius, UNEP/GRID-Arendal](#). Used with permission.

# Net Terrestrial Productivity Record



Total biogenic productivity was only 76-83% of today during the last glacial period!

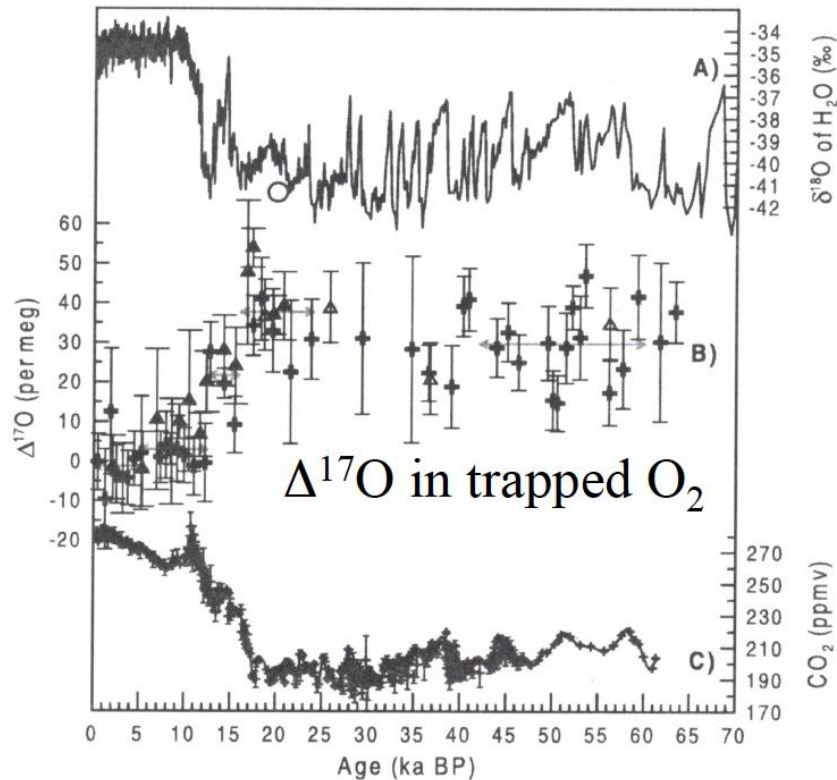
Note that two processes compete: 1) During LGM less CO<sub>2</sub> was available for exchange reactions, leading to less anomalous O<sub>2</sub> being formed, making  $\Delta^{17}\text{O}$  rise to its biological value (Effect: +70). 2) Biological productivity was lower during the LGM, leading to lower  $\Delta^{17}\text{O}$   
**Process 1) dominated**

Results from the Greenland Ice Sheet Project 2 (GISP2) and Siple Dome ice cores. (a)  $\delta^{18}\text{O}$  of the ice, a proxy for local temperature [Grootes *et al.*, 1993] from the GISP2 ice core, Greenland. (b)  $\Delta^{17}\text{O}$  values, where open triangles are results from Luz *et al.* [1999] and crosses and solid triangles are individual measurements from GISP2 and Siple Dome, respectively.

© John Wiley & Sons. All rights reserved. This content is excluded from our Creative Commons license. For more information, see <http://ocw.mit.edu/help/faq-fair-use/>.

Source: Blunier, Thomas, Bruce Barnett, et al. "Biological Oxygen Productivity During the Last 60,000 Year from Triple Oxygen Isotope Measurements." *Global Biogeochemical Cycles* 16, no. 3 (2002): 3-1-3-13.

# Net Terrestrial Productivity Record



Total biogenic productivity was only 76-83% of today during the last glacial period!

Note that two processes compete: 1) During LGM less CO<sub>2</sub> was available for exchange reactions, leading to less anomalous O<sub>2</sub> being formed, making Δ<sup>17</sup>O rise to its biological value (Effect: +70).

2) Biological productivity was lower during the LGM, leading to lower Δ<sup>17</sup>O

**Process 1) dominated**

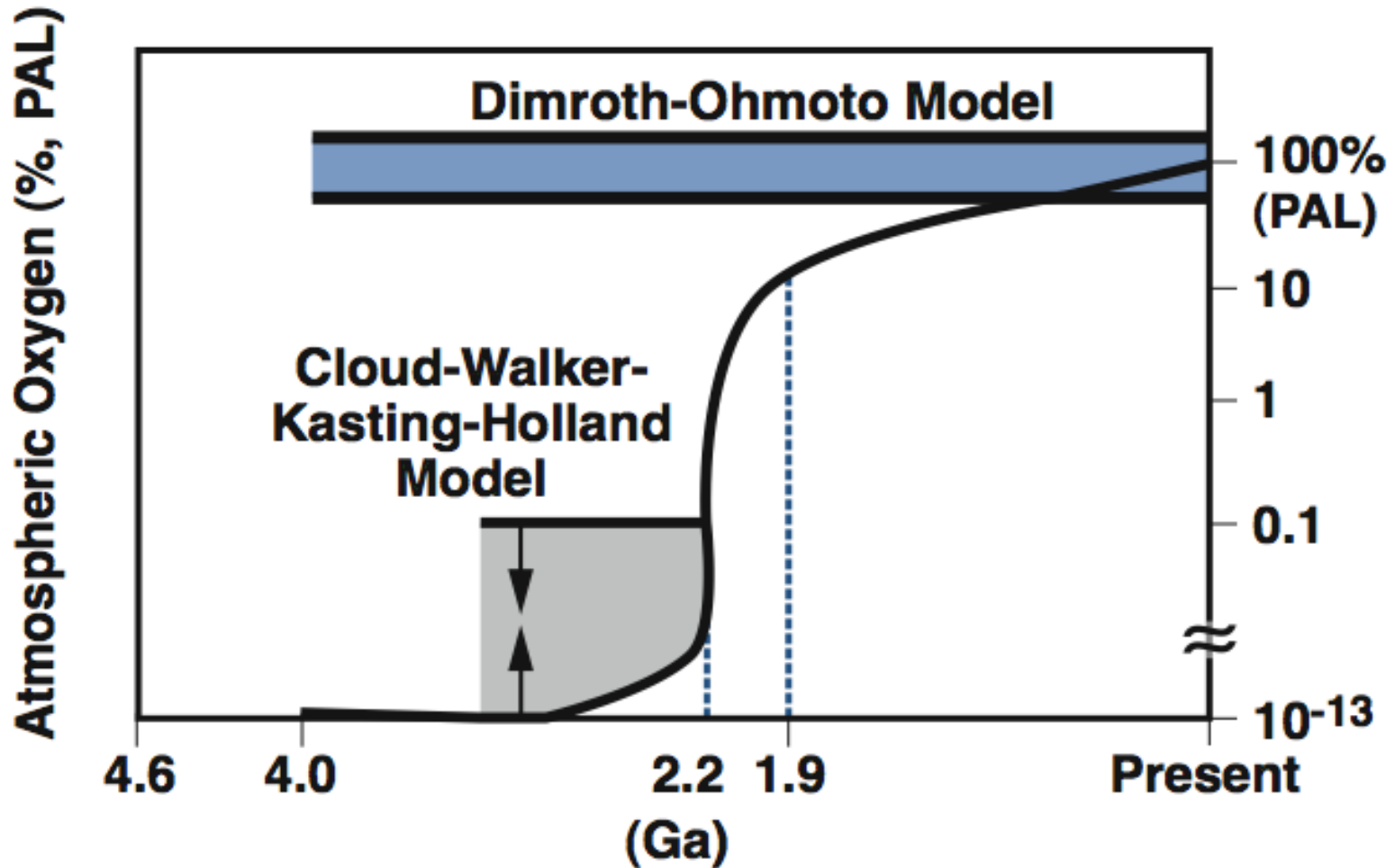
Results from the Greenland Ice Sheet Project 2 (GISP2) and Siple Dome ice cores. (a) δ<sup>18</sup>O of the ice, a proxy for local temperature [Grootes *et al.*, 1993] from the GISP2 ice core, Greenland. (b) Δ<sup>17</sup>O values, where open triangles are results from Luz *et al.* [1999] and crosses and solid triangles are individual measurements from GISP2 and Siple Dome, respectively.

© John Wiley & Sons. All rights reserved. This content is excluded from our Creative Commons license. For more information, see <http://ocw.mit.edu/help/faq-fair-use/>.

Source: Blunier, Thomas, Bruce Barnett, et al. "Biological Oxygen Productivity During the Last 60,000 Year from Triple Oxygen Isotope Measurements." *Global Biogeochemical Cycles* 16, no. 3 (2002): 3-1-3-13.

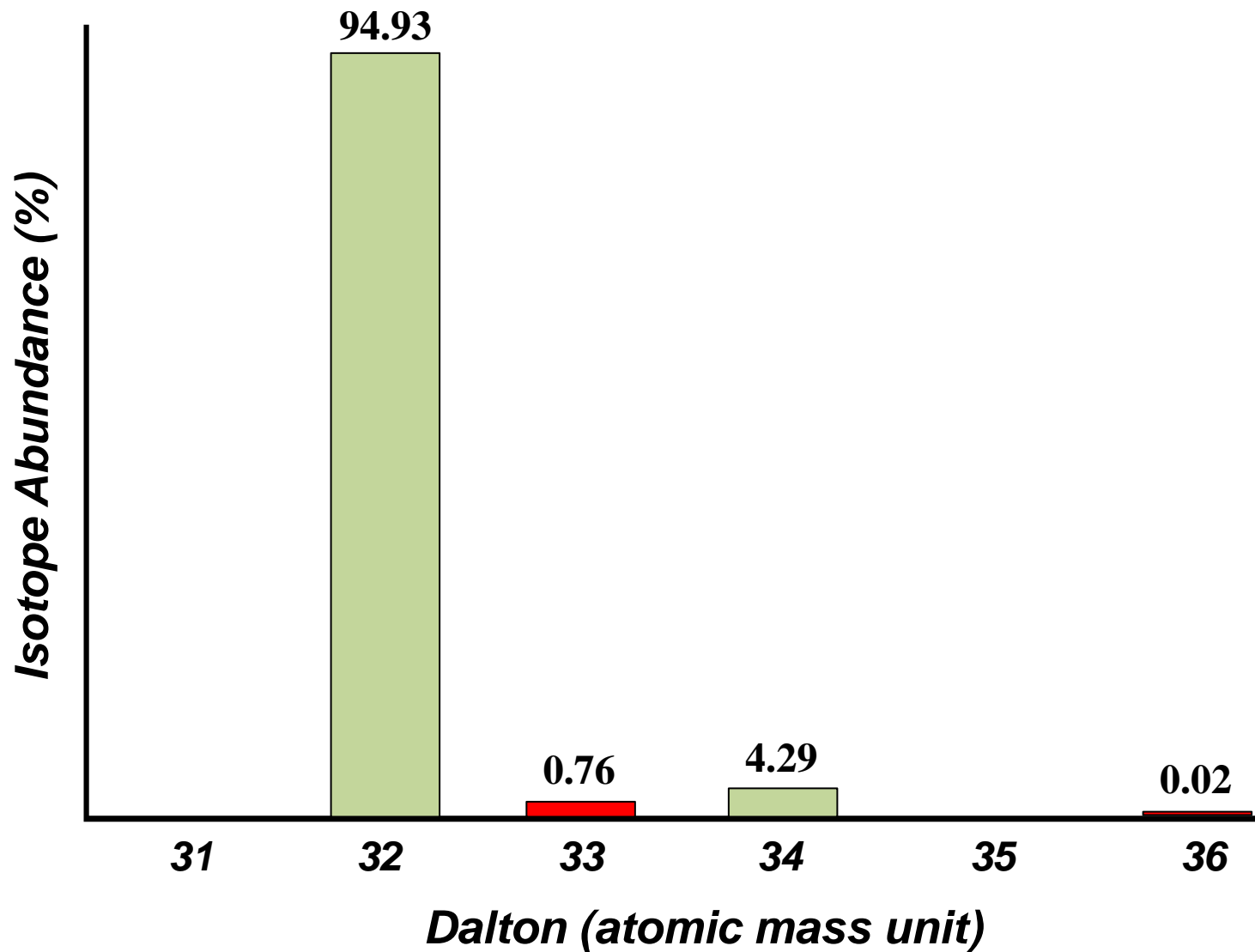
## Two contrasting models for the evolution of atmospheric O<sub>2</sub>

from Ohmoto, Geochem. News #93, Fall 1997

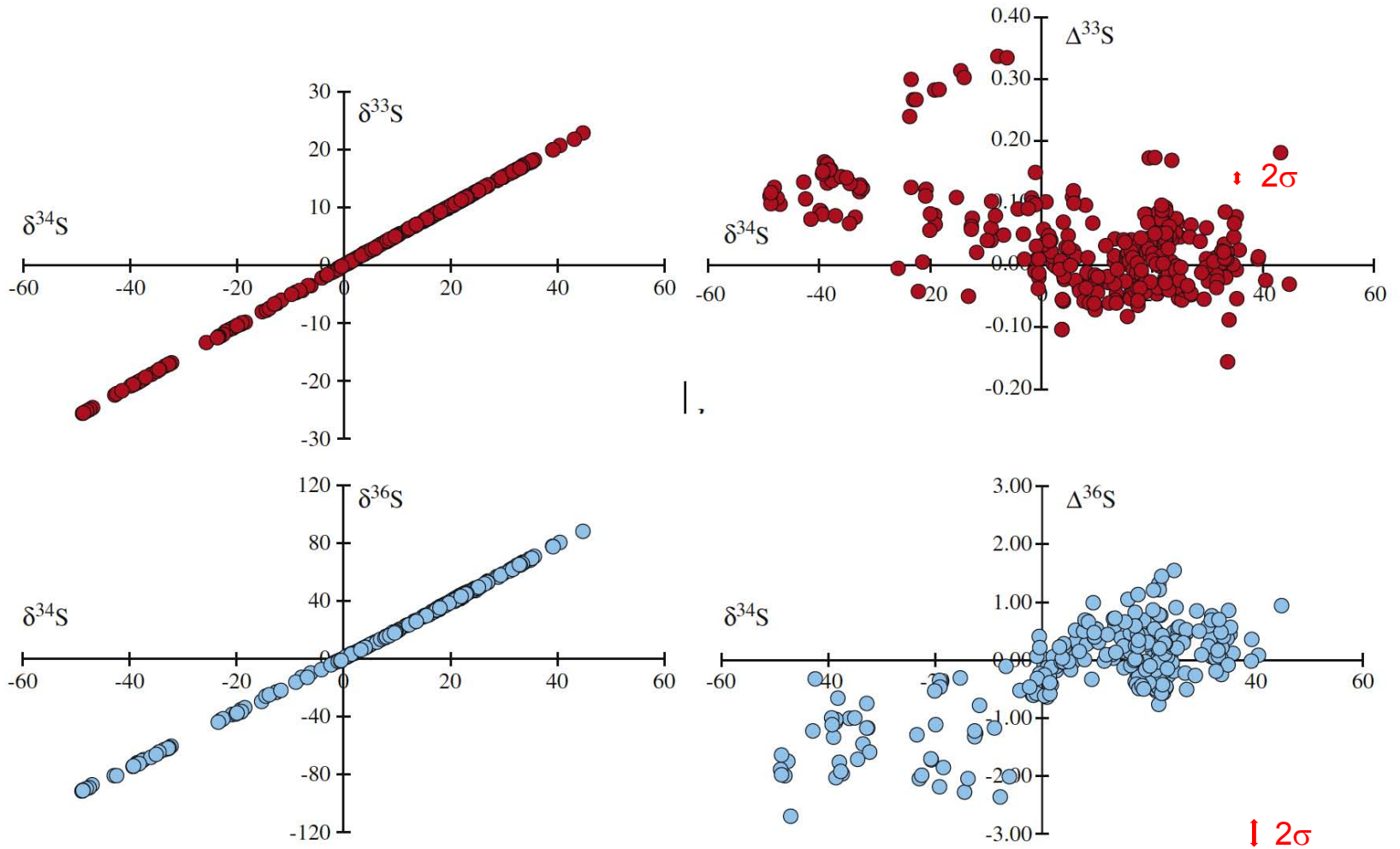


© Geochemical Society. All rights reserved. This content is excluded from our Creative Commons license. For more information, see <http://ocw.mit.edu/help/faq-fair-use/>.

# Stable Sulfur Isotopes



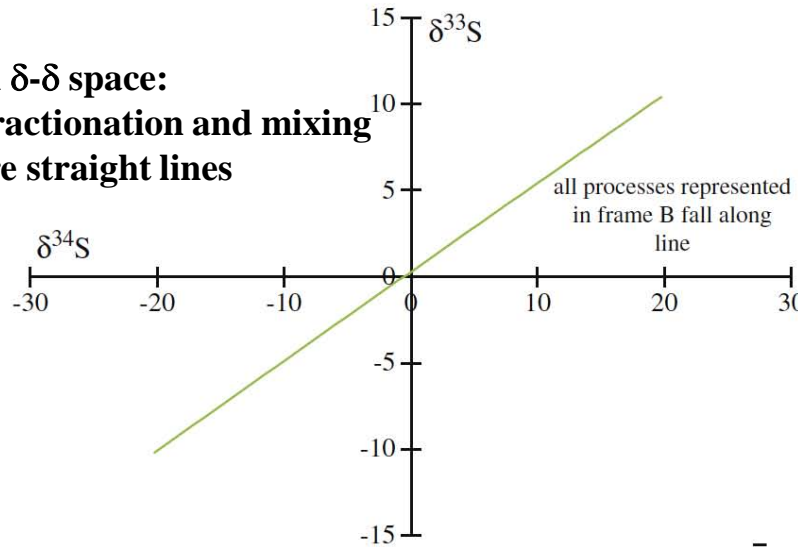
# Conventional vs. Modern mass spectrometry



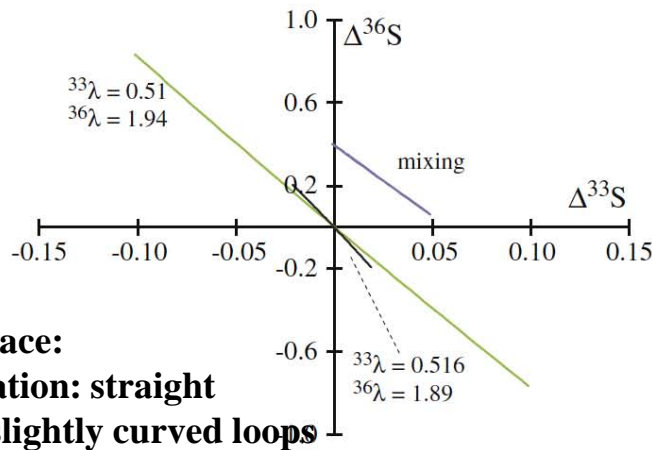
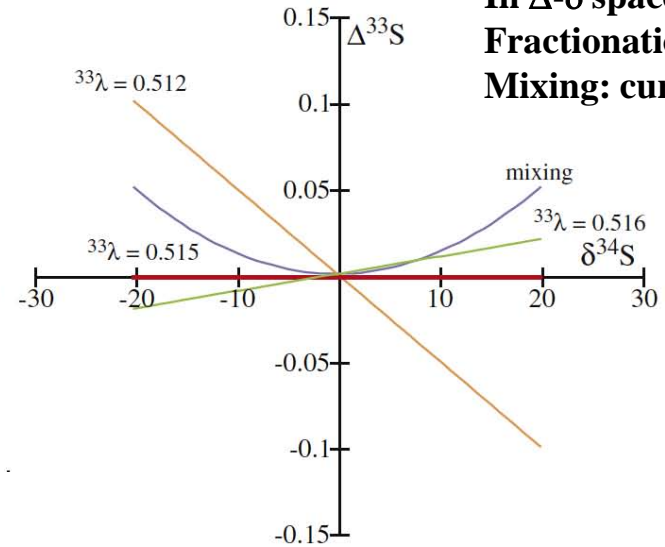
© Elsevier. All rights reserved. This content is excluded from our Creative Commons license. For more information, see <http://ocw.mit.edu/fairuse>. Source: Figure 2 of Johnston, David T. "Multiple Sulfur Isotopes and the Evolution of Earth's Surface Sulfur Cycle." *Earth-Science Reviews* 106, no. 1 (2011): 161-83.

# Slopes of Fractionation and Mixing Trends

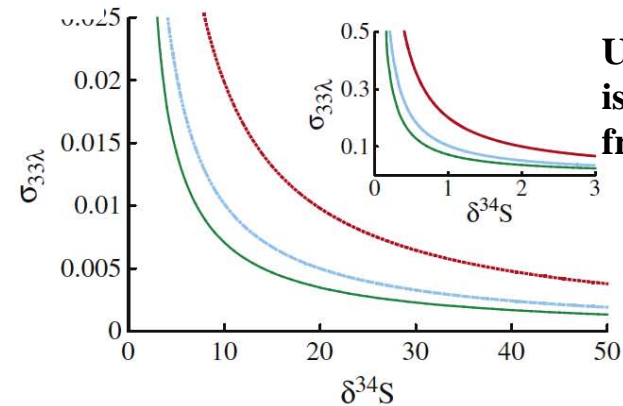
**In  $\delta$ - $\delta$  space:  
Fractionation and mixing  
are straight lines**



**In  $\Delta$ - $\delta$  space:  
Fractionation: straight  
Mixing: curved**



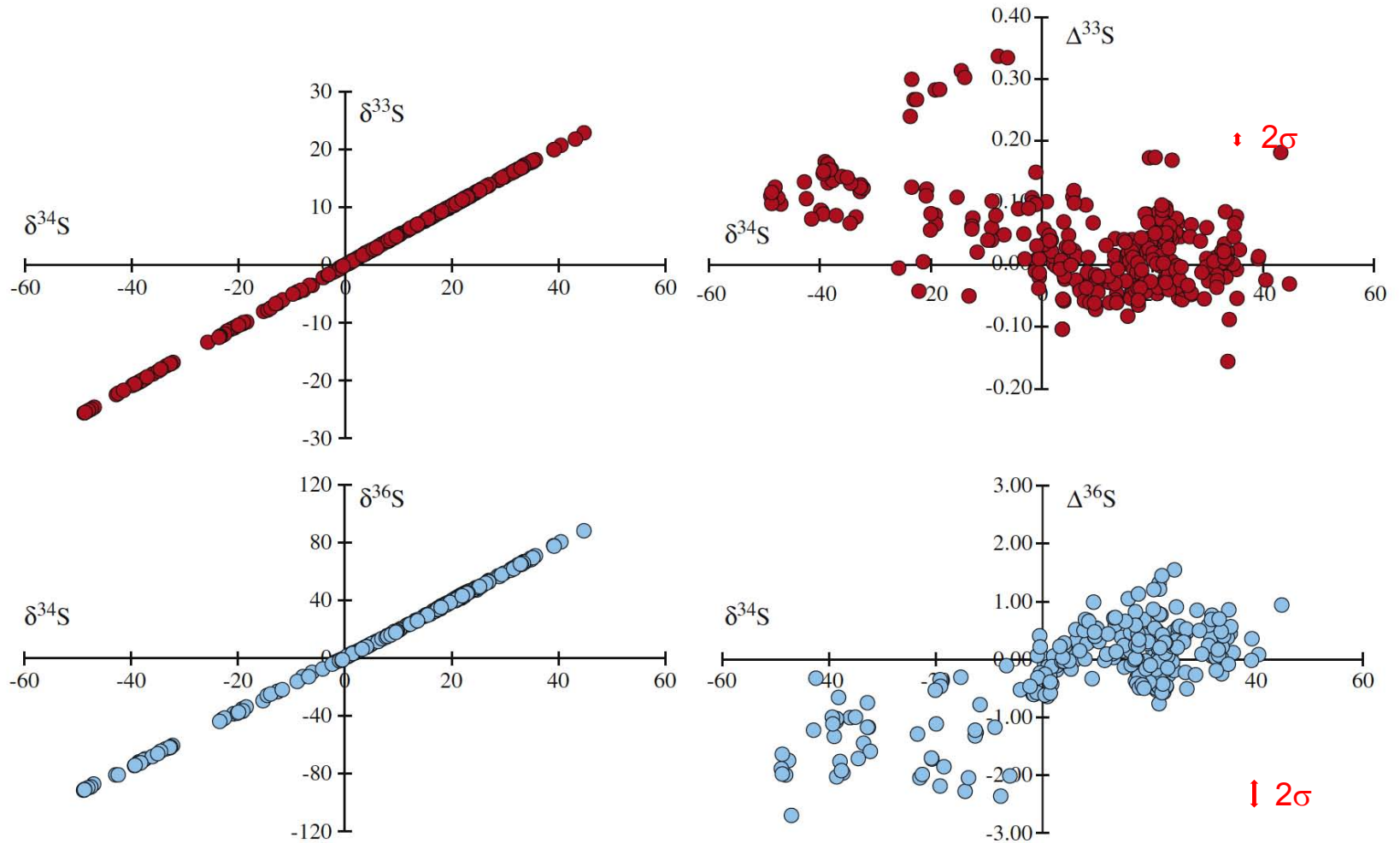
**In  $\Delta$ - $\Delta$  space:  
Fractionation: straight  
Mixing: slightly curved loops**



**Uncertainty ( $\sigma$ )  
is a function of  
fractionation**

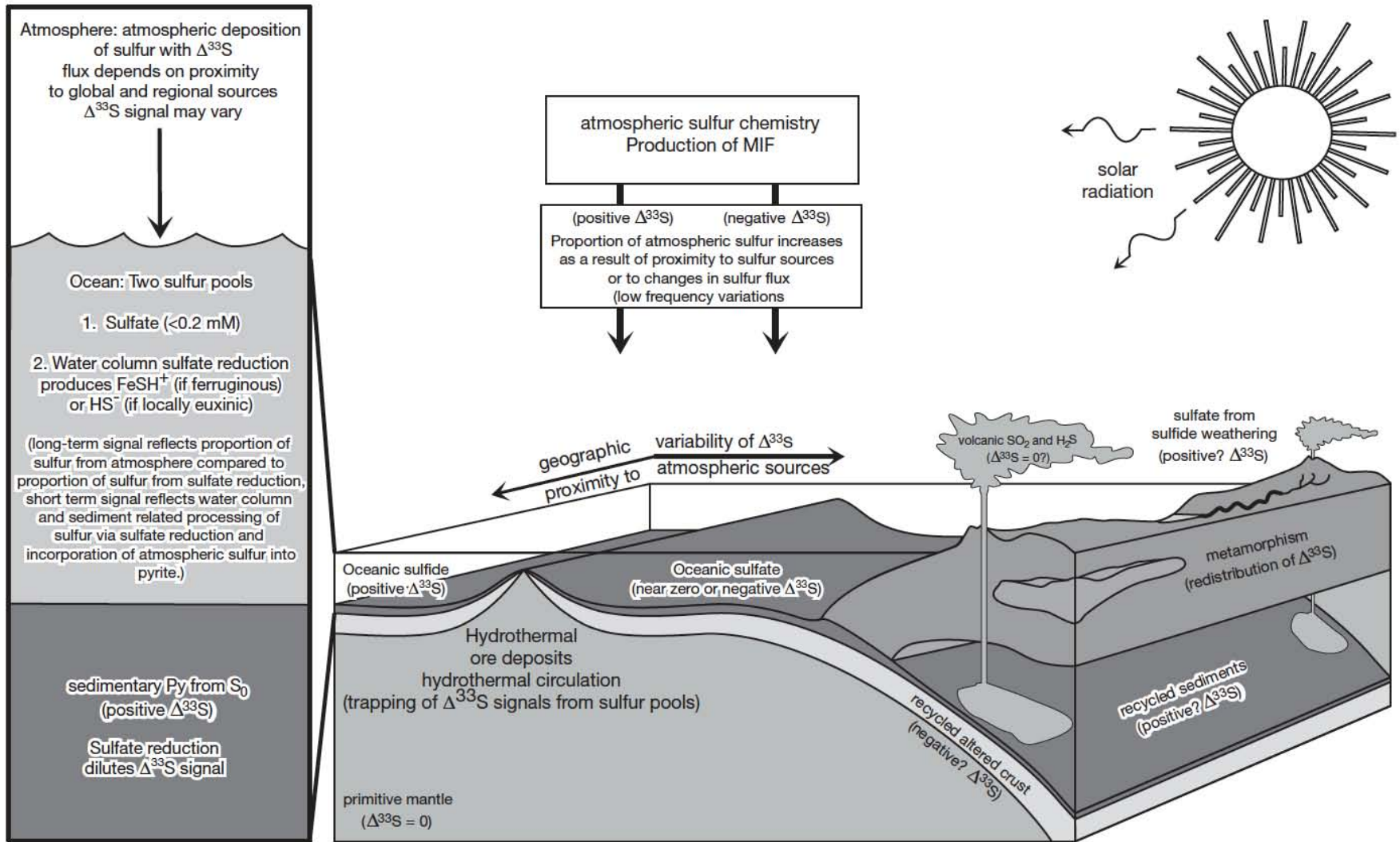
© Elsevier. All rights reserved. This content is excluded from our Creative Commons license. For more information, see <http://ocw.mit.edu/fairuse>. Source: Figure 2 of Johnston, David T. "Multiple Sulfur Isotopes and the Evolution of Earth's Surface Sulfur Cycle." *Earth-Science Reviews* 106, no. 1 (2011): 161-83.

# Conventional vs. Modern mass spectrometry



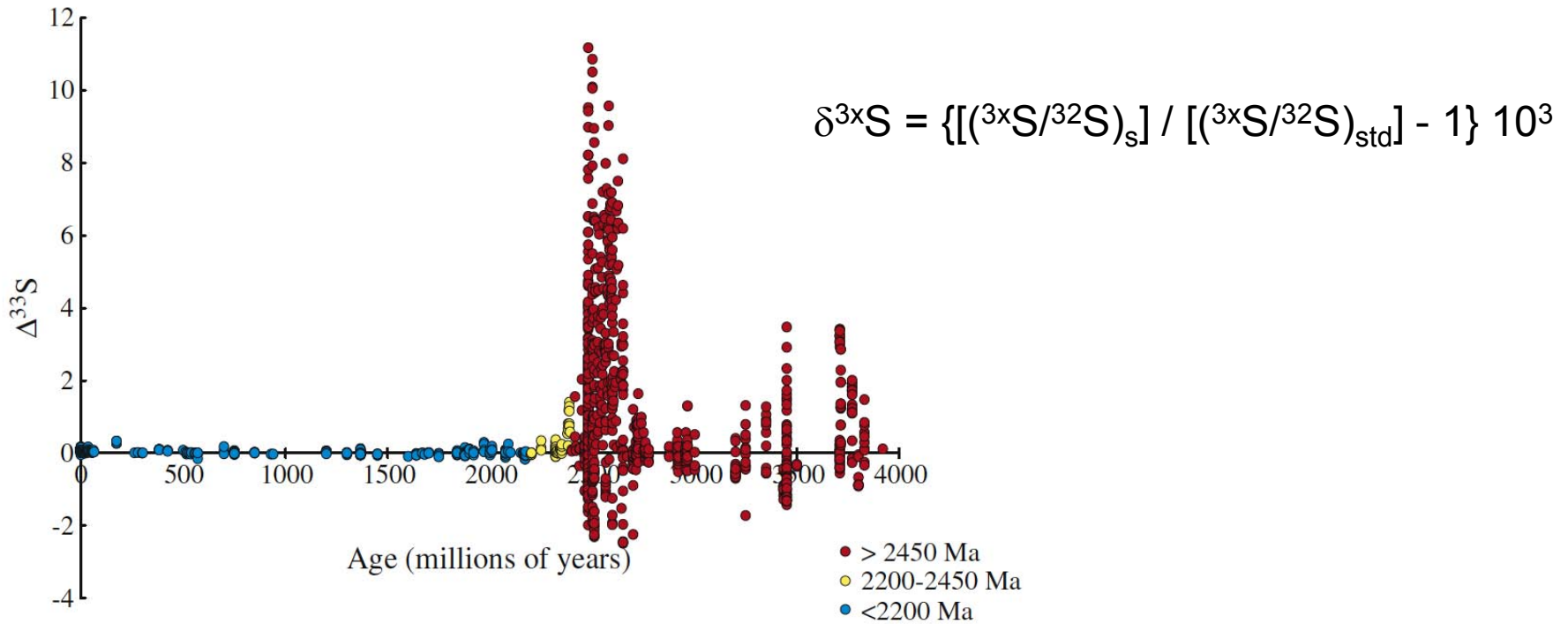
© Elsevier. All rights reserved. This content is excluded from our Creative Commons license. For more information, see <http://ocw.mit.edu/fairuse>. Source: Figure 2 of Johnston, David T. "Multiple Sulfur Isotopes and the Evolution of Earth's Surface Sulfur Cycle." *Earth-Science Reviews* 106, no. 1 (2011): 161-83.

# Processes Affecting the Sulfur Isotope Cycle



© Society of Economic Geologists, Inc. All rights reserved. This content is excluded from our Creative Commons license. For more information, see <http://ocw.mit.edu/fairuse>. Source: Figure 5 in Farquhar, James, Nanping Wu, et al. "Connections between Sulfur Cycle Evolution, Sulfur Isotopes, Sediments, and Base Metal Sulfide Deposits." *Economic Geology* 105, no. 3 (2010): 509-33.

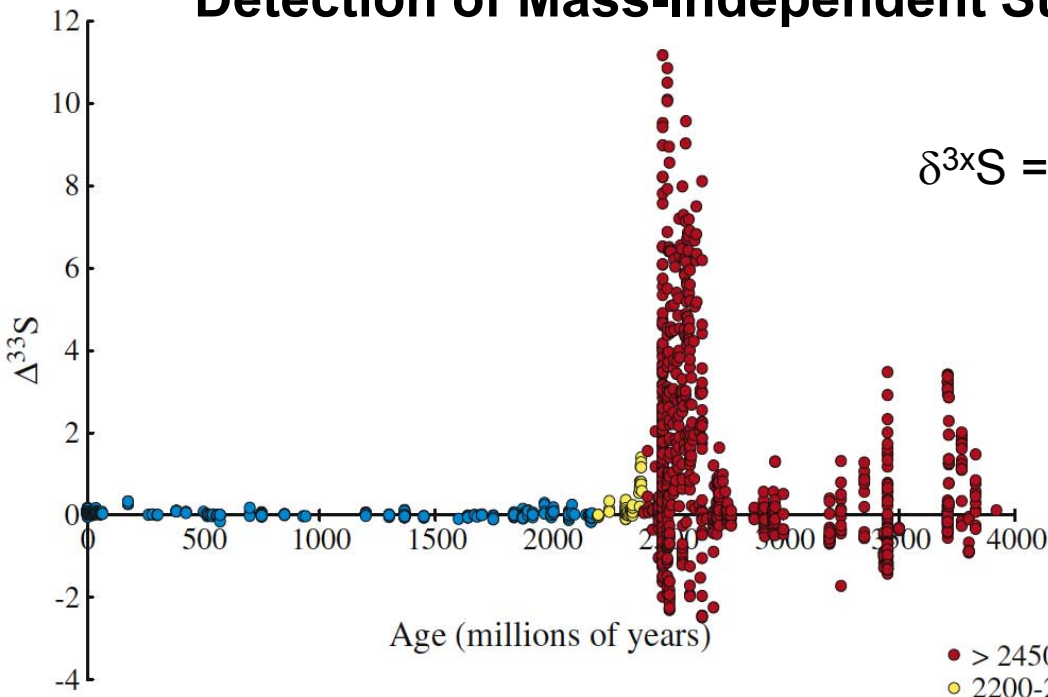
# Detection of Mass-Independent Sulfur Isotope Variations



© Elsevier. All rights reserved. This content is excluded from our Creative Commons license. For more information, see <http://ocw.mit.edu/fairuse>.

Source: Figure 2 of Johnston, David T. "Multiple Sulfur Isotopes and the Evolution of Earth's Surface Sulfur Cycle." *Earth-Science Reviews* 106, no. 1 (2011): 161-83.

# Detection of Mass-Independent Sulfur Isotope Variations



$$\delta^{3xS} = \left\{ \left[ \left( \frac{^{3xS}}{^{32S}} \right)_s / \left( \frac{^{3xS}}{^{32S}} \right)_{std} \right] - 1 \right\} 10^3$$

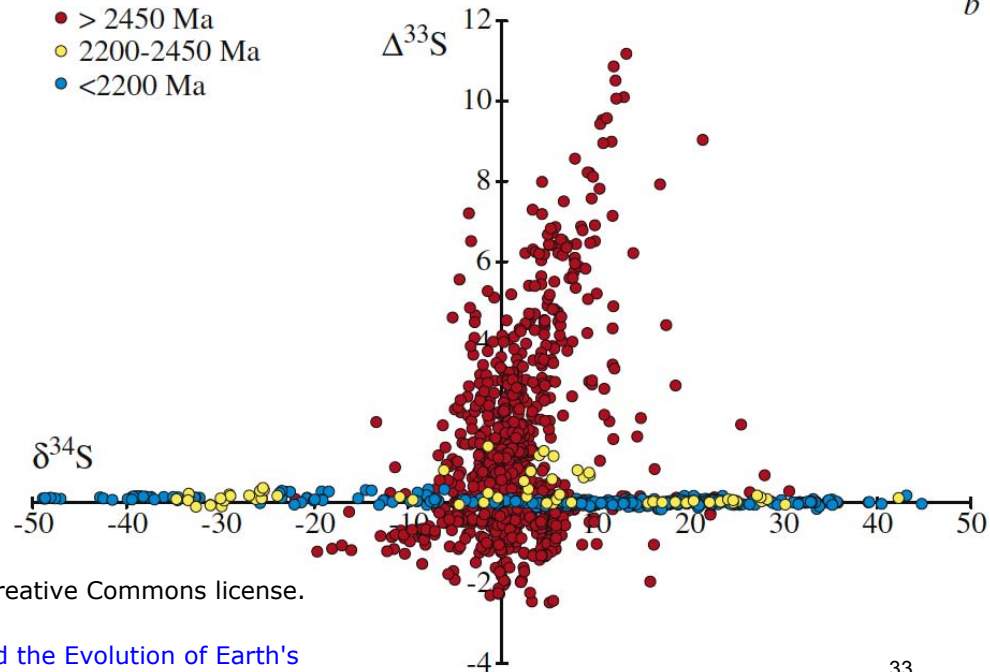
$$\Delta^{3xS} = \delta^{3xS} - 3x\lambda \delta^{34S}$$

$$\lambda = (1/m_1 - 1/m_2) / (1/m_1 - 1/m_3)$$

$$m_1 = 32, m_2 = 33, m_3 = 34$$

(use exact masses)

- > 2450 Ma
- 2200-2450 Ma
- < 2200 Ma



© Elsevier. All rights reserved. This content is excluded from our Creative Commons license. For more information, see <http://ocw.mit.edu/fairuse>.

Source: Figure 2 of Johnston, David T. "Multiple Sulfur Isotopes and the Evolution of Earth's Surface Sulfur Cycle." *Earth-Science Reviews* 106, no. 1 (2011): 161-83.

## Definition of Mass-Independent Sulfur Isotope Variations

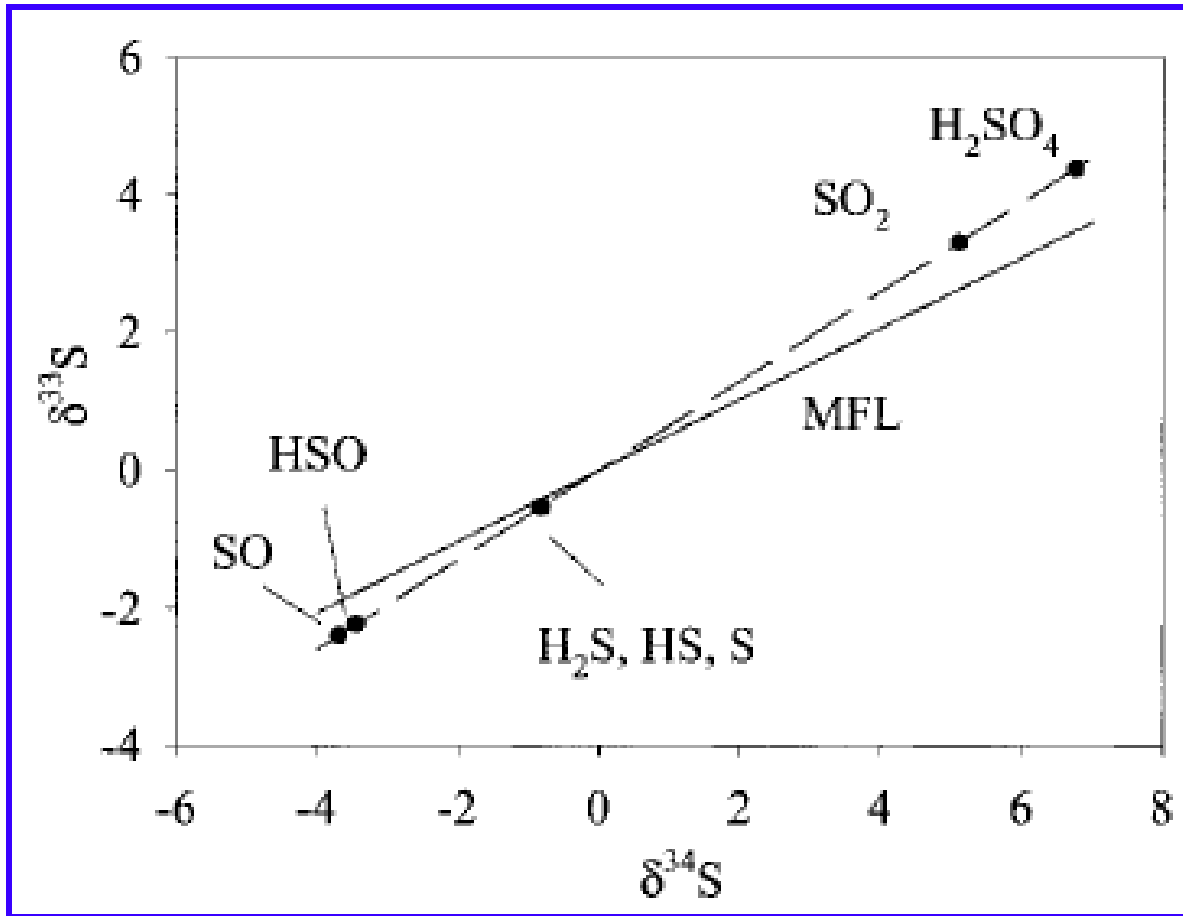
$$\Delta^{3x}S = \delta^{3x}S - 1000 \times \left[ \left( 1 + \frac{\delta^{34}S}{1000} \right)^{3x\lambda} - 1 \right]$$

$$\Delta^{3x}S = 1000 \times \left[ \ln \left( 1 + \frac{\delta^{3x}S}{1000} \right) - 3x\lambda \times \ln \left( 1 + \frac{\delta^{34}S}{1000} \right) \right]$$

These two expressions yield very similar solutions for the range of Earth materials ( $\delta^{34}S$  variations between -5% and 5%).  $\lambda$  can be solved by measuring fractionations, even if the processes involve multiple steps.

$${}^{3x}\lambda = \frac{\ln \left( 1 + \frac{\delta^{3x}S_A}{1000} \right) - \ln \left( 1 + \frac{\delta^{3x}S_B}{1000} \right)}{\ln \left( 1 + \frac{\delta^{34}S_A}{1000} \right) - \ln \left( 1 + \frac{\delta^{34}S_B}{1000} \right)}$$

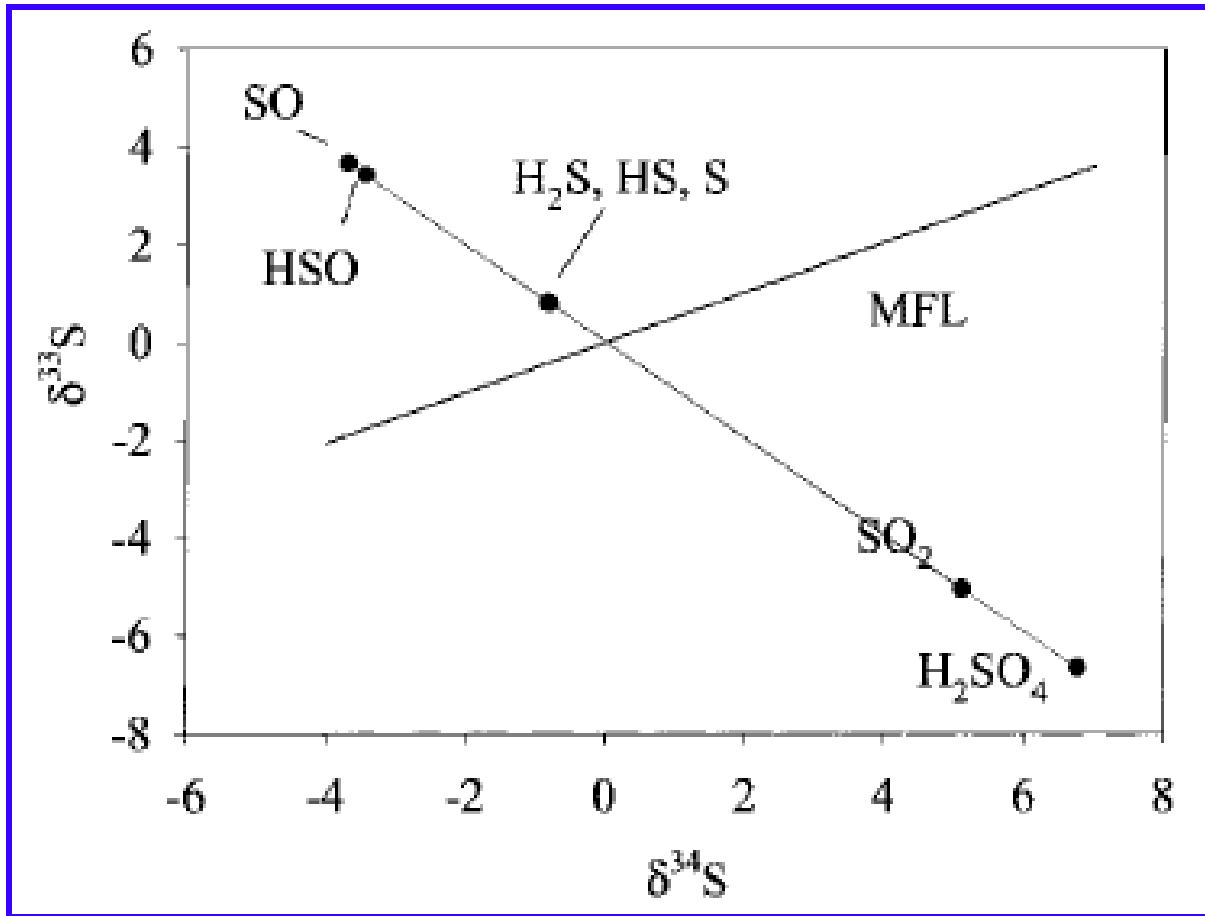
# Stratospheric Photolyses Reactions



Courtesy of Mary Ann Liebert, Inc. Used with permission.

Source: Pavlov, A. A., and J. F. Kasting. "Mass-Independent Fractionation of Sulfur Isotopes in Archean Sediments: Strong Evidence for an Anoxic Archean Atmosphere." *Astrobiology* 2, no. 1 (2002): 27-41.

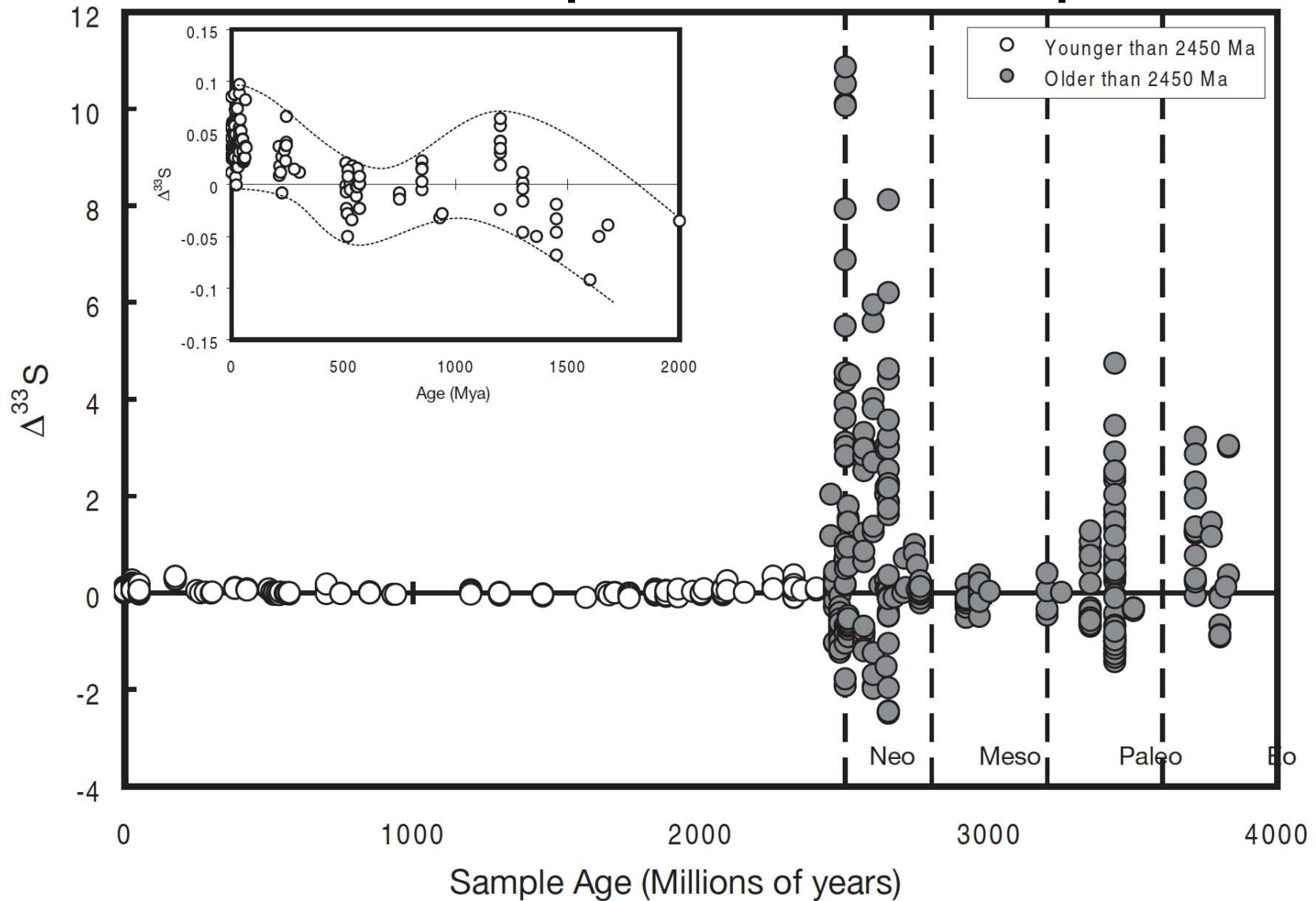
# Stratospheric Photolyses Reactions



Courtesy of Mary Ann Liebert, Inc. Used with permission.

Source: Pavlov, A. A., and J. F. Kasting. "Mass-Independent Fractionation of Sulfur Isotopes in Archean Sediments: Strong Evidence for an Anoxic Archean Atmosphere." *Astrobiology* 2, no. 1 (2002): 27-41.

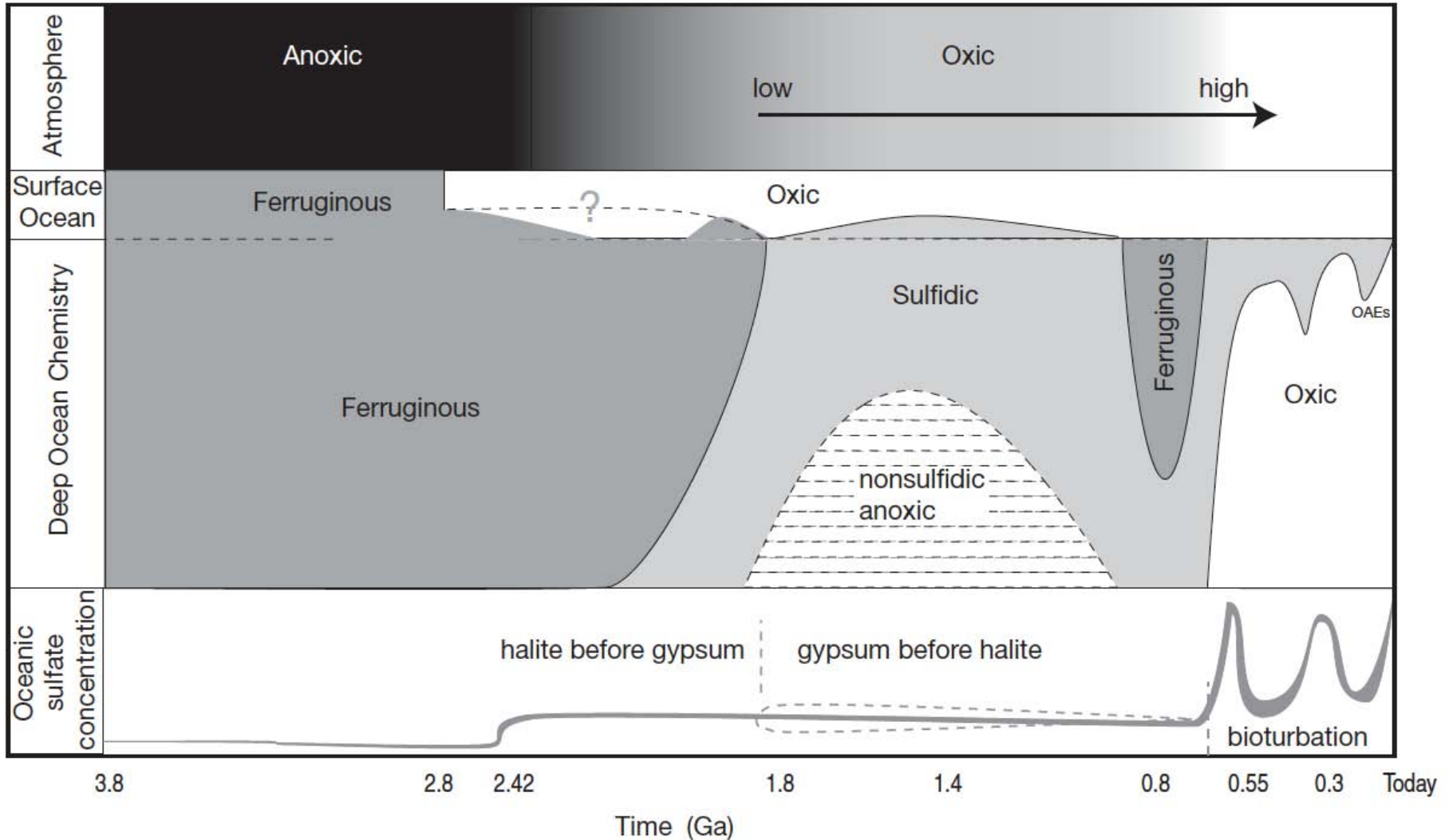
# Record of Mass-Independent Sulfur Isotope Variations



© Society of Economic Geologists, Inc. All rights reserved. This content is excluded from our Creative Commons license. For more information, see <http://ocw.mit.edu/fairuse>.

Source: Figure 5 in Farquhar, James, Nanping Wu, et al. "Connections between Sulfur Cycle Evolution, Sulfur Isotopes, Sediments, and Base Metal Sulfide Deposits." *Economic Geology* 105, no. 3 (2010): 509-33.

# Ideas and Models of Oxygenation of Atmosphere and Ocean



© Society of Economic Geologists, Inc. All rights reserved. This content is excluded from our Creative Commons license.

For more information, see <http://ocw.mit.edu/fairuse>.

Source: Figure 5 in Farquhar, James, Nanping Wu, et al. "Connections between Sulfur Cycle Evolution, Sulfur Isotopes, Sediments, and Base Metal Sulfide Deposits." *Economic Geology* 105, no. 3 (2010): 509-33.

MIT OpenCourseWare  
<http://ocw.mit.edu>

12.744 Marine Isotope Chemistry  
Fall 2012

For information about citing these materials or our Terms of Use, visit: <http://ocw.mit.edu/terms>.